

## ORIGINAL RESEARCH ARTICLE



# Inositol 1,4,5-Trisphosphate Receptor 1 Gain-of-Function Increases the Risk for Cardiac Arrhythmias in Mice and Humans

Bo Sun<sup>1</sup>, Mingke Ni<sup>2</sup>, Yanhui Li<sup>3</sup>, Zhenpeng Song<sup>4</sup>, Hui Wang<sup>5</sup>, Hai-Lei Zhu, MD, PhD; Jinhong Wei, PhD; Darrell Belke, PhD; Shitian Cai, MSc; Wenting Guo, PhD; Jinjing Yao, PhD; Shanshan Tian, MSc; John Paul Estill, MD; Ruiwu Wang, PhD; Mads Toft Søndergaard, PhD; Malene Brohus, PhD; Palle Duun Rohde, PhD; Yongxin Mu, PhD; Alexander Vallmitjana, PhD; Raul Benitez, PhD; Leif Hove-Madsen, PhD; Michael Toft Overgaard, PhD; Glenn I. Fishman, MD; Ju Chen, PhD; Shubhayan Sanatani, MD; Arthur A.M. Wilde, MD, PhD; Michael Fill, PhD; Josefina Ramos-Franco, MD, PhD; Mette Nyegaard, PhD; S.R. Wayne Chen, PhD

**BACKGROUND:**  $\text{Ca}^{2+}$  mishandling in cardiac Purkinje cells is a well-known cause of cardiac arrhythmias. The Purkinje cell resident inositol 1,4,5-trisphosphate receptor 1 (ITPR1) is believed to play an important role in  $\text{Ca}^{2+}$  handling, and ITPR1 gain-of-function (GOF) has been implicated in cardiac arrhythmias. However, nearly all known disease-associated ITPR1 variants are loss-of-function and are primarily linked to neurological disorders. Whether ITPR1 GOF has pathological consequences, such as cardiac arrhythmias, is unclear. This study aimed to identify human ITPR1 GOF variants and determine the impact of ITPR1 GOF on  $\text{Ca}^{2+}$  handling and arrhythmia susceptibility.

**METHODS:** There are a large number of rare ITPR1 missense variants reported in open data repositories. Based on their locations in the ITPR1 channel structure, we selected and characterized 33 human ITPR1 missense variants from open databases and identified 21 human ITPR1 GOF variants. We generated a mouse model carrying a human ITPR1 GOF variant, ITPR1-W1457G (W1447G in mice).

**RESULTS:** We showed that the ITPR1-W1447G<sup>+/−</sup> and recently reported ITPR1-D2594K<sup>+/−</sup> GOF mutant mice were susceptible to stress-induced ventricular arrhythmias. Confocal  $\text{Ca}^{2+}$  and voltage imaging in situ in heart slices and  $\text{Ca}^{2+}$  imaging and patch-clamp recordings of isolated Purkinje cells showed that ITPR1-W1447G<sup>+/−</sup> and ITPR1-D2594K<sup>+/−</sup> variants increased the occurrence of stress-induced spontaneous  $\text{Ca}^{2+}$  release, delayed afterdepolarization, and triggered activity in Purkinje cells. To assess the potential role of ITPR1 variants in arrhythmia susceptibility in humans, we looked up a gene-based association study in the UK Biobank data set and identified 7 rare ITPR1 missense variants showing potential association with cardiac arrhythmias. Remarkably, in vitro functional characterization revealed that all these 7 ITPR1 variants resulted in GOF.

**CONCLUSIONS:** Our studies in mice and humans reveal that enhanced function of *ITPR1*, a well-known movement disorder gene, increases the risk for cardiac arrhythmias.

**Key Words:** cardiac ryanodine receptor ■ inositol 1,4,5-trisphosphate receptor ■ Purkinje cells ■ sarcoplasmic reticulum ■ spontaneous  $\text{Ca}^{2+}$  release ■ triggered activity ■ ventricular arrhythmias

Correspondence to: S.R. Wayne Chen, PhD, 3280 Hospital Dr NW, Calgary, Alberta, Canada, T2N 4N1, Email swchen@ucalgary.ca; Mette Nyegaard, PhD, Department of Health Science and Technology, Aalborg University, Denmark, Email nyegaard@hst.aau.dk; or Bo Sun, PhD, Medical School, Kunming University of Science and Technology, Kunming, 650500, China, Email sunbo1025@hotmail.com

\*B. Sun, M. Ni, and Y. Li contributed equally.

Supplemental Material is available at <https://www.ahajournals.org/doi/suppl/10.1161/CIRCULATIONAHA.124.070563>.

For Sources of Funding and Disclosures, see page 860.

© 2024 The Authors. *Circulation* is published on behalf of the American Heart Association, Inc., by Wolters Kluwer Health, Inc. This is an open access article under the terms of the [Creative Commons Attribution Non-Commercial-NoDerivs](#) License, which permits use, distribution, and reproduction in any medium, provided that the original work is properly cited, the use is noncommercial, and no modifications or adaptations are made.

*Circulation* is available at [www.ahajournals.org/journal/circ](http://www.ahajournals.org/journal/circ)

## Clinical Perspective

### What Is New?

- In vitro analyses identified, from open data repositories, novel gain-of-function variants in the inositol 1,4,5-trisphosphate receptor 1 (ITPR1) gene that has been implicated in cardiac arrhythmias.
- Mouse models with ITPR1 gain-of-function variants exhibited increased spontaneous calcium release, delayed afterdepolarization, triggered activity, and risk of stress-induced ventricular arrhythmias.
- Many rare human ITPR1 gain-of-function variants identified in the UK Biobank data set were associated with an increased risk of cardiac arrhythmias.

### What Are the Clinical Implications?

- *ITPR1*, a well-known movement disorder gene, is also a risk gene for cardiac arrhythmia.
- Consideration should be given to include *ITPR1* gene in clinical genetic testing for cardiac arrhythmias.
- Targeting ITPR1 function may represent a novel therapeutic strategy for reducing cardiac arrhythmia risk.

## Nonstandard Abbreviations and Acronyms

<b>Cntn2</b>	contactin 2
<b>DAD</b>	delayed afterdepolarization
<b>ET-1</b>	endothelin-1
<b>GOF</b>	gain-of-function
<b>IP<sub>3</sub></b>	inositol 1,4,5-trisphosphate
<b>IP<sub>3</sub>BM</b>	myo-inositol 1,4,5-trisphosphate hexakis (butyryloxymethyl)
<b>ITPR1</b>	inositol 1,4,5-trisphosphate receptor 1
<b>RyR2</b>	cardiac ryanodine receptor
<b>SCR</b>	spontaneous Ca <sup>2+</sup> release
<b>VA</b>	ventricular arrhythmia

Inositol 1,4,5-trisphosphate receptor 1 (ITPR1) is an intracellular Ca<sup>2+</sup> release channel located primarily on the sarco/endoplasmic reticulum membrane. It governs the release of Ca<sup>2+</sup> from the intracellular stores in a variety of cells under the control of inositol 1,4,5-trisphosphate (IP<sub>3</sub>), the endogenous ligand that opens Inositol 1,4,5-trisphosphate receptors (ITPRs).<sup>1–4</sup> ITPR1-mediated Ca<sup>2+</sup> release plays an important role in many cellular functions, including movement coordination, learning and memory, muscle contraction, fertilization, gene expression, apoptosis, etc.<sup>5–8</sup> Given its critical roles in numerous signaling pathways, defective ITPR1 function would be expected to contribute to diseases of multiple systems. Surprisingly, naturally occurring mutations in ITPR1 have mainly been associated with neu-

rological disorders, such as spinocerebellar ataxias, seizure, intellectual disability, or Gillespie syndrome.<sup>9–11</sup> The predominant association of ITPR1 with neurological disorders is consistent with the abundant expression of ITPR1 in the brain, especially in the cerebellum.<sup>12–14</sup> Besides the brain, ITPR1 expression is also enriched in many other cells/tissues.<sup>7,15–21</sup> However, the pathological consequences of defective ITPR1 function in other ITPR1-expressing cells/tissues are poorly understood.

In the heart, ITPR1 is predominantly expressed in Purkinje fibers of the cardiac conduction system and only weakly expressed in other areas of the heart.<sup>22–28</sup> In addition to ITPR1, cardiac Purkinje cells also express another intracellular Ca<sup>2+</sup> release channel, RyR2 (cardiac ryanodine receptor). ITPR1- and RyR2-mediated Ca<sup>2+</sup> release plays a major role in Ca<sup>2+</sup> homeostasis in Purkinje cells. It is important to note that Purkinje cell Ca<sup>2+</sup> dysregulation is believed to be a major cause of cardiac arrhythmias.<sup>24,29,30</sup> Enhanced RyR2 function promotes spontaneous sarcoplasmic reticulum Ca<sup>2+</sup> release in Purkinje cells. This spontaneous Ca<sup>2+</sup> release (SCR) in the form of Ca<sup>2+</sup> waves can activate the electrogenic Na<sup>+</sup>/Ca<sup>2+</sup> exchanger and produce delayed afterdepolarizations (DADs). Suprathreshold DADs can evoke triggered activity leading to arrhythmias.<sup>31–36</sup> Indeed, naturally occurring RyR2 gain-of-function (GOF) mutations promote SCR to cause catecholaminergic polymorphic ventricular tachycardia, an inherited arrhythmogenic disorder characterized by physical/emotional stress-induced polymorphic or bidirectional ventricular tachycardias.<sup>36–39</sup> Enhanced ITPR1-mediated Ca<sup>2+</sup> release is also known to significantly contribute to SCR in Purkinje cells.<sup>23,25,28</sup> Given the close link between SCR, DADs, and triggered activity, enhanced ITPR1 function in Purkinje cells may also contribute to stress-induced cardiac arrhythmias. Although the roles of ITPRs in cardiac arrhythmias have been investigated for decades,<sup>40</sup> direct evidence for the involvement of the specific ITPR isoform, ITPR1, in cardiac arrhythmia is lacking.

To specifically assess the role of enhanced ITPR1 function in arrhythmia susceptibility, we performed ECG stress testing on a recently reported ITPR1-D2594K<sup>+/-</sup> GOF mutant mouse model<sup>41</sup> and found that the D2594K<sup>+/-</sup> mutant mice were vulnerable to stress-induced ventricular arrhythmias (VAs).<sup>41</sup> We then identified 28 human ITPR1 GOF mutants from open data repositories and generated a novel mouse model harboring the human ITPR1 GOF variant W1457G (W1447G in mice). The W1447G<sup>+/-</sup> mice also showed susceptibility to stress-induced VAs. We further found that ITPR1 GOF increases the susceptibility to stress-induced VAs by promoting SCR-evoked triggered activity in Purkinje cells. Analysis of the UK Biobank data set further identified human ITPR1 GOF variant carriers with an increased risk of cardiac arrhythmias. Thus, our work suggests that *ITPR1*, a well-known neurological disorder gene, may also be a risk gene for cardiac arrhythmias.

## METHODS

The data supporting the findings of this study are available from the corresponding author upon reasonable request.

### Animal Studies

All animal studies were approved by the institutional animal care and use committees at the University of Calgary and were performed in accordance with US National Institutes of Health guidelines and the Animal Research: Reporting of In Vivo Experiments (ARRIVE) reporting guidelines. Adult (5–8 months of age) genetically engineered ITPR1 mutant mice (ITPR1-W1447G<sup>+/-</sup> and ITPR1-D2594K<sup>+/-</sup>) and wild-type mice of both sexes were used. All animal models were housed in the mouse facility of Cumming School of Medicine, University of Calgary. All animal experiments were performed blind to genotype. Animals were assigned randomly to the experimental groups, and both male and female animals were used in experiments. No animals were excluded from analyses. A minimum sample size ( $n=6$  per group) for animal studies was estimated using the G\*Power3.1 program with an effect size of 2, a significance level ( $\alpha$ ) of 0.05, and power of 0.8. Sample sizes and  $P$  values can be found in the figures and figure legends.

### General Methods

We first searched 5 open data repositories of variants from exome or genome sequenced samples for potential GOF ITPR1 variants. Selected missense variants were functionally characterized using IP<sub>3</sub>-induced Ca<sup>2+</sup> release assays in HEK293 cells. We generated mouse models harboring GOF ITPR1 variants and assessed their susceptibility to stress-induced VAs using pharmacological challenges and ECG recordings. In addition, we established a mouse line expressing both the ITPR1 GOF variant and the Purkinje cell marker contactin 2 (Cntn2)–GFP (green fluorescent protein) to assess Ca<sup>2+</sup> dynamics and membrane potentials in Purkinje cells. To determine the potential role of ITPR1 GOF variants in arrhythmias susceptibility in humans, we exploited a gene-based phenome-wide association analysis performed among 50 000 exome sequenced participants from UK Biobank. The 7 top associated variants were functionally characterized to investigate their impact on IP<sub>3</sub>-induced Ca<sup>2+</sup> release in HEK293 cells. Detailed methods are provided in the [Supplemental Material](#).

### Statistical Analysis

All experiments were performed blind to genotype, age and treatment. Normality of data distribution was assessed using the Shapiro-Wilk test. All data shown are mean $\pm$ SEM unless indicated otherwise. For normally distributed data sets, parametric tests were performed. For non-Gaussian-distributed data sets, nonparametric methods were used. With respect to nonparametric analyses, the Mann-Whitney  $U$  test (2-sided) was used for 2 groups; the Kruskal-Wallis test with Dunn post hoc test was used for  $\geq 3$  groups. The Wilcoxon signed-rank test was used for paired samples. With respect to parametric analyses, the Student  $t$  test (2-sided) was used for 2 groups; 1-way ANOVA followed by the Tukey post hoc test was used for  $\geq 3$  groups. The  $\chi^2$  test was used to determine significant differences in frequencies between different groups. The paired  $t$  test was used for paired samples. Statistical analyses were

performed using GraphPad Prism 8 (GraphPad Software). Hierarchical statistical analysis was performed in RStudio. Details can be found in the supplemental methods. Sample sizes and  $P$  values can be found in figure legends or figures.  $P$  values  $<0.05$  were considered statistically significant.

## RESULTS

### Identification of ITPR1 GOF Variants in Humans

To assess the potential association between ITPR1 GOF and VAs, we searched for ITPR1 GOF variants in humans. To date, there are many known disease-linked ITPR1 variants reported in the literature<sup>9–11,42,43</sup> and in ClinVar (<https://www.ncbi.nlm.nih.gov/clinvar/>). There are also hundreds of rare ITPR1 missense variants reported in the public data repositories ([Table S1](#)). However, the functional ramifications of most of these ITPR1 rare variants are unknown. In contrast, many disease-associated RyR2 mutations are known to cause GOF, and a majority of these are clustered in disease-mutation hotspots<sup>36</sup> ([Figure 1A](#)). Given the structural and functional homology between ITPRs and RyRs, we focused on ITPR1 variants located in regions corresponding to the known RyR2 disease-mutation hotspots. Using this screening strategy, we identified 33 human ITPR1 variants ([Figure 1B through 1D](#); [Table S1](#)). Each of these variants was expressed in HEK293 cell lines, and the median effective concentration (EC<sub>50</sub>) to IP<sub>3</sub> activation was measured and compared with the wild type (WT) ([Figure 1B and 1C](#); [Table S1](#); [Figure S1](#)). This comparative functional analysis revealed 21 GOF and 6 loss-of-function ITPR1 variants as well as 6 variants with WT-like function. The GOF phenotypes of some ITPR1 variants were confirmed using the Inositol 1,4,5-trisphosphate receptor null human embryonic kidney 293 (HEK-3KO) cells in which all 3 ITPR isoforms have been knocked out ([Figure S2](#)). These in vitro functional analyses indicate that ITPR1 GOF variants exist in humans.

### ITPR1 GOF Increases the Susceptibility to Stress-Induced VAs in Mice

To determine whether human ITPR1 GOF variants increase the susceptibility to stress-induced VAs, we generated a mouse model harboring the human ITPR1-W1457G<sup>+/-</sup> (mouse W1447G<sup>+/-</sup>) GOF variant ([Figure 2](#)). This variant is located in the central domain of the ITPR1 channel, which corresponds to a known RyR2 disease hotspot ([Figure 1A](#)).<sup>36</sup> The mouse W1447G<sup>+/-</sup> variant markedly increased the sensitivity of ITPR1 to IP<sub>3</sub> activation (EC<sub>50</sub>=26 nM compared with the 59 nM of WT channels;  $P<0.0001$ ; [Figure 2](#); [Table S1](#)).

We then assessed the susceptibility of the ITPR1-W1447G<sup>+/-</sup> (human W1457G<sup>+/-</sup>) mice to stress-induced VAs by performing ECG recordings before and after administering a mixture of epinephrine and caffeine, a commonly used method for inducing VAs in mouse

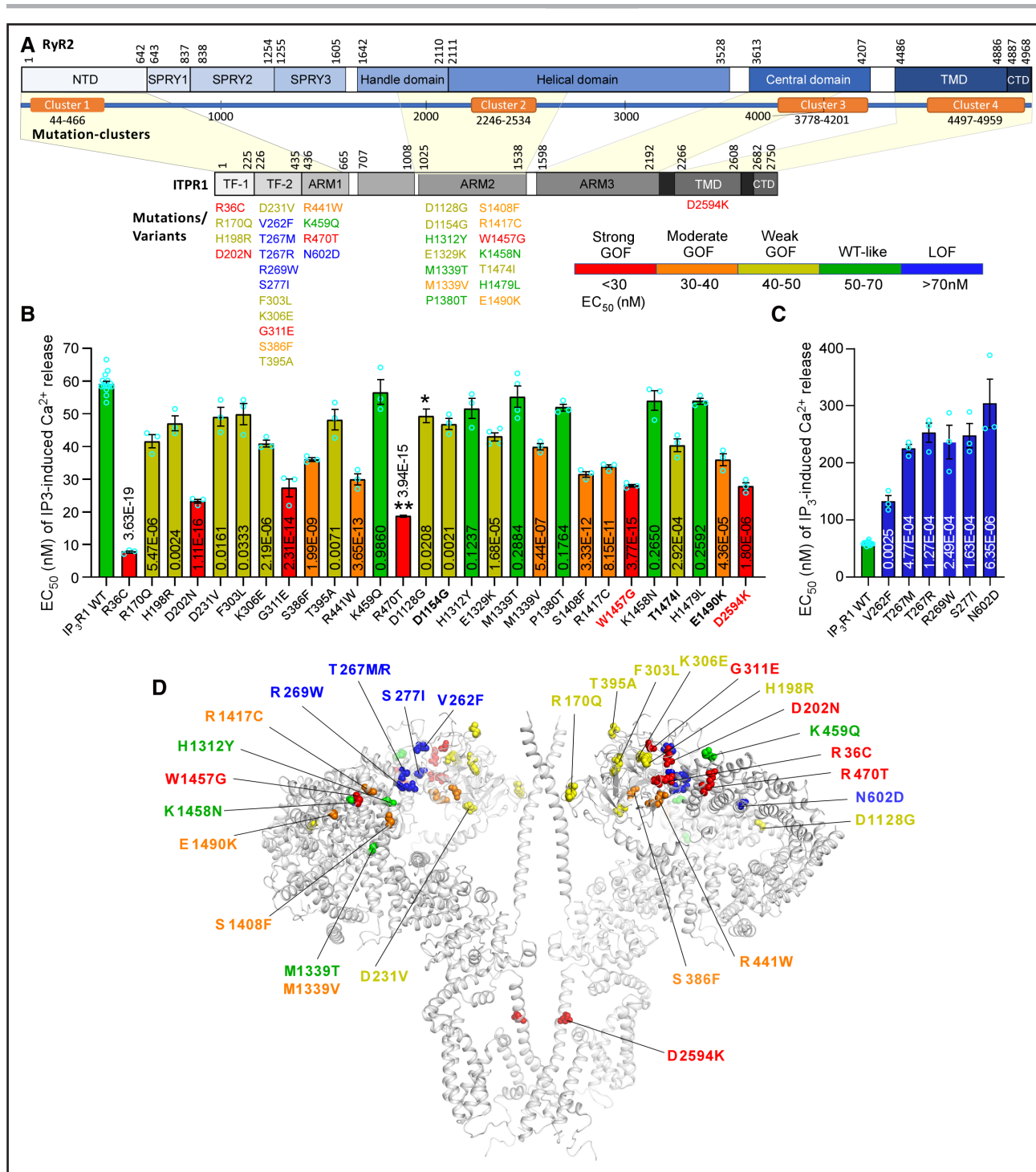


**Figure 1. Identification, location, and in vitro functional characterization of human ITPR1 variants.**

**A**, Schematic diagram of the linear sequences of RyR2 and ITPR1. Major domains of RyR2 are shown as solid blue boxes. The orange boxes indicate 4 disease-associated mutation clusters (hotspots) of RyR2. Major domains of ITPR1 are shown as solid gray/black boxes. The corresponding homologous regions of ITPR1 and RyR2 are indicated by yellow-shaded areas. Human ITPR1 variants characterized are grouped under domains they reside in and are color-coded as those shown in **B** and **C**. **B** and **C**,  $EC_{50}$  values of  $IP_3$  induced  $Ca^{2+}$  release in HEK293 cells expressing ITPR1 WT or mutants with the range of  $EC_{50}$  values color-coded. Data shown are mean  $\pm$  SEM ( $n=3$  or  $4$ ; 1-way ANOVA with Dunnett post hoc test for obtaining  $P$  values shown in **B** and **C**). Three ITPR1 variants, D1154G, T1474I, and E1490K, are also present in the UK Biobank. **D**, Locations of ITPR1 variants in the 3-dimensional structure of ITPR1 (PDB: 6MU2). The ITPR1-D2594K mutation was generated in our structure-function relationship analysis of the channel pore (not a human variant). The 3-dimensional structural locations of ITPR1 variants, D1154G, E1329K, P1380T, T1474I, and H1479L, have not been resolved and thus were not shown in the 3-dimensional structure (**D**). GOF indicates gain-of-function; and LOF, loss-of-function.





HEK293 cells expressing ITPR1-WT (**A**) and the human ITPR1-W1457G mutant (**B**) were transfected with an ER luminal fluorescent  $\text{Ca}^{2+}$ -sensing protein, G-CEPIA1er. Representative traces of ER  $\text{Ca}^{2+}$  (G-CEPIA1er) signals at baseline (0  $\text{IP}_3$ ), after addition of different concentrations of  $\text{IP}_3$  (10–300 nM), and after addition of 1  $\mu\text{M}$   $\text{IP}_3$  plus 4  $\mu\text{M}$  CPA are shown. **C**, The dose-response curves of  $\text{IP}_3$ -induced fractional  $\text{Ca}^{2+}$  release in ITPR1 WT and ITPR1-W1457G mutant cells were determined by measuring the signal drop in ER  $\text{Ca}^{2+}$  level after a given  $\text{IP}_3$  dose and normalized to the total ER  $\text{Ca}^{2+}$  store (the drop in ER  $\text{Ca}^{2+}$  level after addition of 1  $\mu\text{M}$   $\text{IP}_3$  plus 4  $\mu\text{M}$  CPA). Data shown are mean  $\pm$  SEM ( $n=3$ ; 1-way ANOVA with Dunnett post hoc test for obtaining  $P$  values shown in **C**). **D**, Location of residue ITPR1-W1447 in exon 34 of the mouse *itpr1* gene and the crRNA and PAM sequences used for the CRISPR-mediated mutagenesis of the  $\text{IP}_3\text{R1-W1447G}$  mutation. **E**, Sequence of the single-strand oligodeoxynucleotides (ssODNs) used for homologous DNA repair. **F**, Genotyping of the ITPR1-W1447G mutant allele using PCR. **G**, Confirmation of the W1447G $^{+/-}$  mutation in heterozygous mouse samples by DNA sequencing.

models.<sup>44–49</sup> ITPR1-W1447G<sup>+/-</sup> GOF mutant mice displayed significantly increased duration and inducibility of VA, especially bidirectional ventricular tachycardia, compared with ITPR1-WT mice (Figure 3A through 3D; Table S2). Bidirectional ventricular tachycardia was not observed when epinephrine or isoproterenol were administered without caffeine (Table S2). It is also important to note that the expression level of the ITPR1 protein in the ITPR1-WT and ITPR1-W1447G<sup>+/-</sup> GOF mutant hearts was similar (Figure S3).

We also performed ECG recordings on the ITPR1-D2594K<sup>+/-</sup> GOF mutant mice that we recently reported,<sup>41</sup> both before and after injection of a mixture of epinephrine and caffeine. Like ITPR1-W1447G <sup>+/-</sup> GOF mice, the ITPR1-D2594K<sup>+/-</sup> GOF mice also exhibited stress-induced VAs with significantly increased VA duration and inducibility compared with WT mice (Figure 3E through 3H; [Table S2](#)). Taken together, these results show that ITPR1 GOF increases the susceptibility to stress-induced VAs in mice.

We next investigated how enhanced ITPR1 function increases the propensity for stress-induced VAs in mice. It is well-established that under stress conditions, en-

hanced RyR2 function increases the propensity for spontaneous  $\text{Ca}^{2+}$  waves, which in turn promotes DADs and triggered activity in Purkinje fibers and consequently stress-induced VAs.<sup>44,50–54</sup> Because ITPR1 is primarily expressed in Purkinje fibers in the heart,<sup>22–28</sup> enhanced ITPR1 function may contribute to  $\text{Ca}^{2+}$  waves, DADs, and triggered activity in Purkinje fibers. Purkinje fibers are located in the subendocardium and constitute only a very small proportion of cells in the heart. To be able to specifically identify and study Purkinje fibers in the heart, we used a mouse model expressing the Cntn2-GFP, a specific marker for Purkinje fibers.<sup>53,55</sup> We cross-bred the ITPR1mGOF mice with the Cntn2-GFP mice to produce the Cntn2-GFP/ITPR1-W1447G<sup>+/-</sup>, Cntn2-GFP/ITPR1-D2594K<sup>+/-</sup>, and Cntn2-GFP/ITPR1-WT mice.

To assess the effect of ITPR1 GOF on intracellular  $\text{Ca}^{2+}$  handling in Purkinje fibers, heart slices were prepared and loaded with Rhod-2 acetoxymethyl (AM) esters for confocal in situ  $\text{Ca}^{2+}$  imaging. Under baseline conditions (ie, in the absence of epinephrine and caffeine), Cntn2-GFP-labeled ITPR1-WT Purkinje fibers or ITPR1-WT ventricular myocytes in heart slices displayed few or no spontaneous  $\text{Ca}^{2+}$  waves (Figure S4A, S4D, S4E, and S4H). In contrast, spontaneous  $\text{Ca}^{2+}$  waves were readily observed in Cntn2-GFP-labeled ITPR1-W1447G<sup>+/-</sup> and -D2594K<sup>+/-</sup> Purkinje fibers under baseline conditions (Figure S4B through S4D). To determine the impact of ITPR1 GOF on intracellular

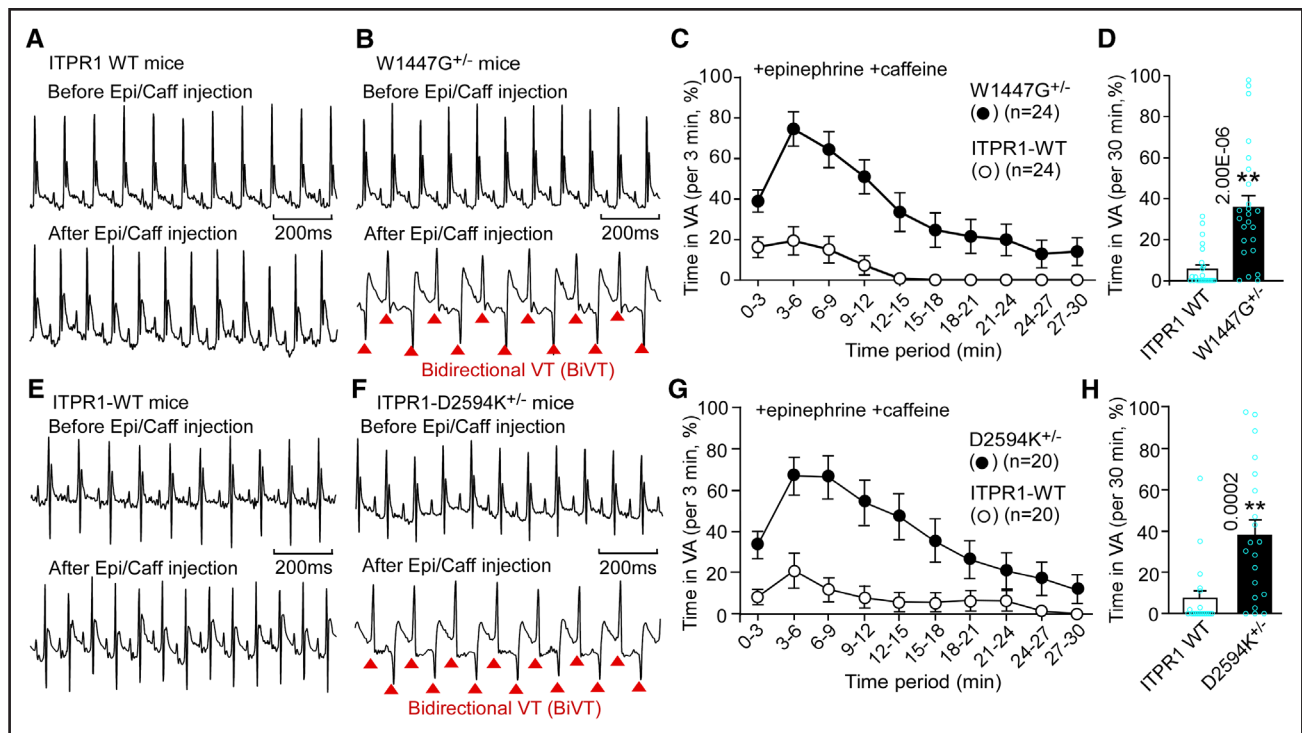


**Figure 3. ITPR1 GOF increases the susceptibility to stress-induced VAs in mice.**

Representative ECG recordings of WT (A) and W1447G<sup>+/−</sup> (human W1457G) mutant (B) mice before and after injection of epinephrine (1.6 mg/kg) and caffeine (120 mg/kg). VA duration (%) in WT and W1447G<sup>+/−</sup> mice within each 3-minute (C) or 30-minute (D) period of ECG recordings. Data shown are mean±SEM (n=24 for WT, and 24 for W1447G<sup>+/−</sup>; Mann-Whitney U test for obtaining P values shown in D). Representative ECG recordings of ITPR1-WT (E) and ITPR1-D2594K<sup>+/−</sup> (F) mice before and after injection of epinephrine (1.6 mg/kg) and caffeine (120 mg/kg). VA duration (%) in ITPR1-WT and ITPR1-D2594K<sup>+/−</sup> mice within each 3-minute (G) or 30-minute (H) period of ECG recordings. Data shown are mean±SEM (n=20 for ITPR1-WT and 20 for ITPR1-D2594K<sup>+/−</sup>; Mann-Whitney U test for obtaining P values shown in H). Bidirectional ventricular tachycardias (BiVTs) displaying beat-to-beat alternations in QRS morphology and axis are indicated by red arrowheads.

Ca<sup>2+</sup> handling specifically in ventricular myocytes without the influence by neighboring Purkinje cells, we selected ventricular myocytes in an area without the presence of neighboring Cntn2-GFP-labeled Purkinje cells in heart slices for confocal Ca<sup>2+</sup> imaging. It is interesting that, unlike Purkinje fibers, there were few or no spontaneous Ca<sup>2+</sup> waves in ITPR1-W1447G<sup>+/−</sup> or -D2594K<sup>+/−</sup> ventricular myocytes in heart slices (Figure S4F through S4H), which is consistent with the low level of ITPR1 expression in ventricular myocytes.<sup>22–28</sup>

Under stress conditions (ie, during epinephrine and caffeine challenge), the frequencies of spontaneous Ca<sup>2+</sup> waves were markedly increased in Cntn2-GFP-labeled ITPR1-W1447G<sup>+/−</sup> and ITPR1-D2594K<sup>+/−</sup> Purkinje fibers (Figure 4A through 4E) but not in ITPR1-D2594K<sup>+/−</sup> and ITPR1-W1447G<sup>+/−</sup> ventricular myocytes (Figure 4F through 4I). On the other hand, Cntn2-GFP-labeled ITPR1-WT Purkinje fibers or ITPR1-WT ventricular myocytes in heart slices showed few or no spontaneous Ca<sup>2+</sup> waves in the presence of epinephrine and caffeine (Figure 4A, 4B, 4E, 4F, and 4I).

We also determined the effect of ITPR1 GOF on Ca<sup>2+</sup> transient properties. There were no major differences in the amplitude or decay time of Ca<sup>2+</sup> transients in Purkinje fibers or ventricular myocytes between Cntn2-GFP/

ITPR1-WT and -W1447G<sup>+/−</sup> or -D2594K<sup>+/−</sup> heart slices in the absence or presence of epinephrine/caffeine (Figure S5). Taken together, our data show that enhanced ITPR1 function increases the propensity for stress-induced spontaneous Ca<sup>2+</sup> waves in Purkinje fibers, but not in ventricular myocytes.

### ITPR1-W1447G<sup>+/−</sup> GOF Variant Increases Spontaneous Ca<sup>2+</sup> Release in Isolated Purkinje Cells

To further investigate the arrhythmogenic mechanism of ITPR1 GOF in Purkinje fibers, we assessed the effect of the ITPR1-W1447G<sup>+/−</sup> GOF variant on spontaneous Ca<sup>2+</sup> release at the level of isolated Cntn2-GFP-labeled Purkinje cells using confocal line scanning Ca<sup>2+</sup> imaging. We found that, under baseline conditions, there was no significant difference in the frequency of Ca<sup>2+</sup> waves between isolated Cntn2-GFP/ITPR1-W1447G<sup>+/−</sup> and Cntn2-GFP/ITPR1-WT Purkinje cells (Figure 5A, 5C, and 5E), whereas, the frequency of Ca<sup>2+</sup> sparks in isolated Cntn2-GFP/ITPR1-W1447G<sup>+/−</sup> Purkinje cells was significantly increased compared with isolated Cntn2-GFP/ITPR1-WT cells (Figure 5A, 5C, and 5F). On the other hand, under stress conditions, the frequencies of Ca<sup>2+</sup> waves and Ca<sup>2+</sup>

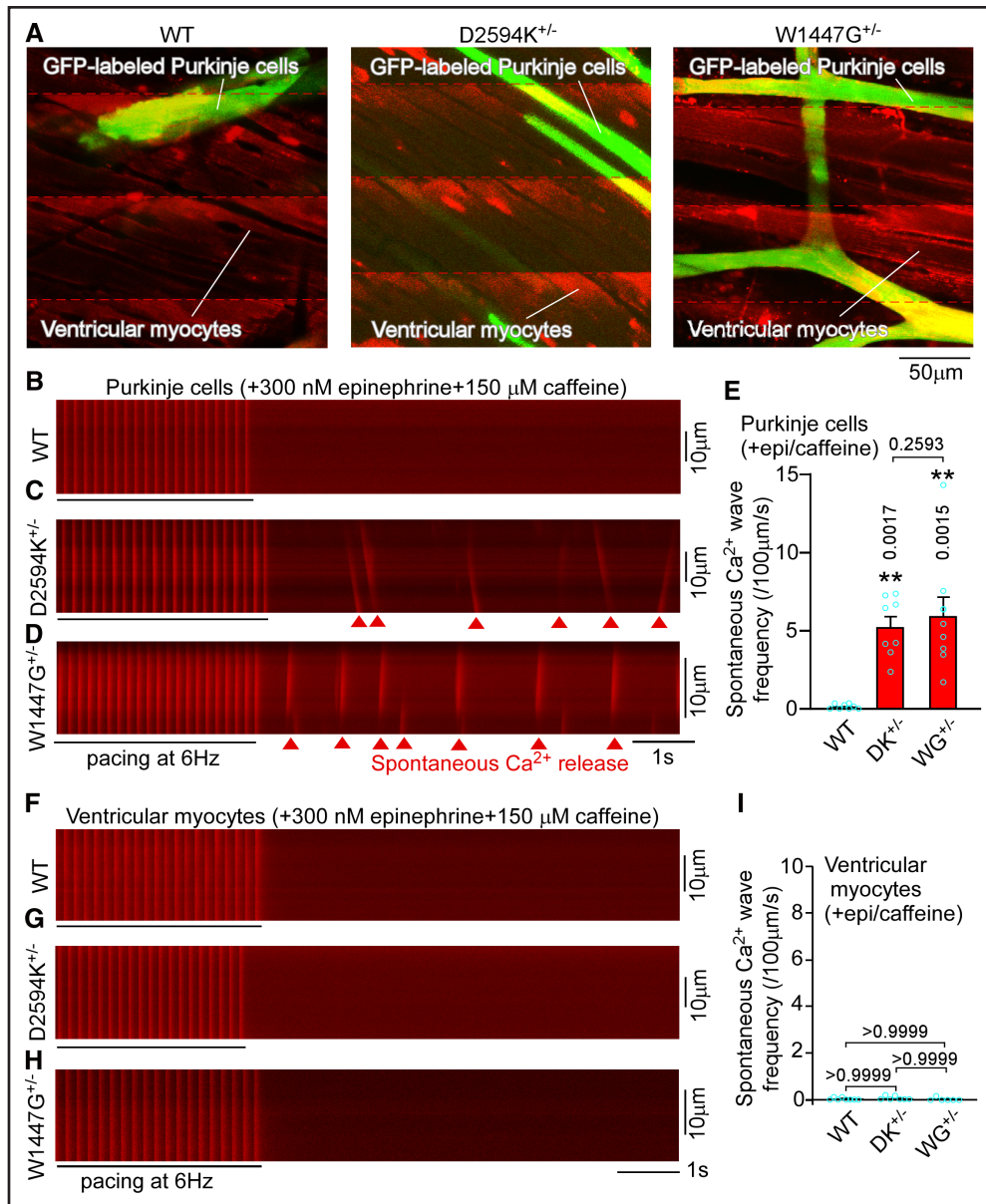


**Figure 4. ITPR1 GOF variants increase spontaneous  $\text{Ca}^{2+}$  release in Purkinje fibers but not in ventricular myocytes in heart slices.**

Confocal x-y images of Cntn2-GFP/ITPR1-WT (left), Cntn2-GFP/ITPR1-D2594K<sup>+/-</sup> (middle), and Cntn2-GFP/ITPR1-W1447G<sup>+/-</sup> (right) mouse heart slices loaded with Rhod-2 AM, showing the GFP-labeled Purkinje fibers and Rhod-2 AM-loaded Purkinje fibers and ventricular myocytes (A). The red dashed lines indicate the occurrence of pacing-induced  $\text{Ca}^{2+}$  transients. Heart slices were perfused with 300 nM epinephrine and 150  $\mu\text{M}$  caffeine.  $\text{Ca}^{2+}$  dynamics (Rhod-2 signals) in ITPR1-WT (B), ITPR1-D2594K<sup>+/-</sup> (C), and ITPR1-W1447G<sup>+/-</sup> (D) Cntn2-GFP-labeled Purkinje fibers and in ITPR1-WT (F), ITPR1-D2594K<sup>+/-</sup> (G), and ITPR1-W1447G<sup>+/-</sup> (H) ventricular myocytes were recorded using line-scanning confocal imaging during electrical field stimulation (6 Hz; indicated by a black line) and after the cessation of stimulation. Frequency of spontaneous  $\text{Ca}^{2+}$  waves in ITPR1-WT, ITPR1-D2594K<sup>+/-</sup>, and ITPR1-W1447G<sup>+/-</sup> Cntn2-GFP-labeled Purkinje fibers (E) and ventricular myocytes (I) in the presence of epinephrine and caffeine. Data shown are mean  $\pm$  SEM (n=8 hearts for ITPR1-WT, 8 hearts for ITPR1-D2594K<sup>+/-</sup>, and 9 hearts for ITPR1-W1447G<sup>+/-</sup>; Kruskal-Wallis test with Dunn post hoc test for obtaining the adjusted *P* values shown in E and I).

sparks in isolated Cntn2-GFP/ITPR1-W1447G<sup>+/-</sup> Purkinje cells were markedly increased compared with those in isolated Cntn2-GFP/ITPR1-WT Purkinje cells (Figure 5B, 5D, 5E, and 5F). Furthermore, ryanodine treatment (10  $\mu\text{M}$ ) abolished these spontaneous  $\text{Ca}^{2+}$  waves and  $\text{Ca}^{2+}$  sparks (Figure S6), revealing a critical role of RyR2 in

these spontaneous  $\text{Ca}^{2+}$  release events. Moreover, the sarcoplasmic reticulum  $\text{Ca}^{2+}$  content did not differ between Cntn2-GFP/ITPR1-WT and Cntn2-GFP/ITPR1-W1447G<sup>+/-</sup> Purkinje cells, as revealed by caffeine-induced  $\text{Ca}^{2+}$  release and the integrated  $\text{Na}^{+}/\text{Ca}^{2+}$  exchanger current measurements (Figures S7 and S8). Therefore, ITPR1



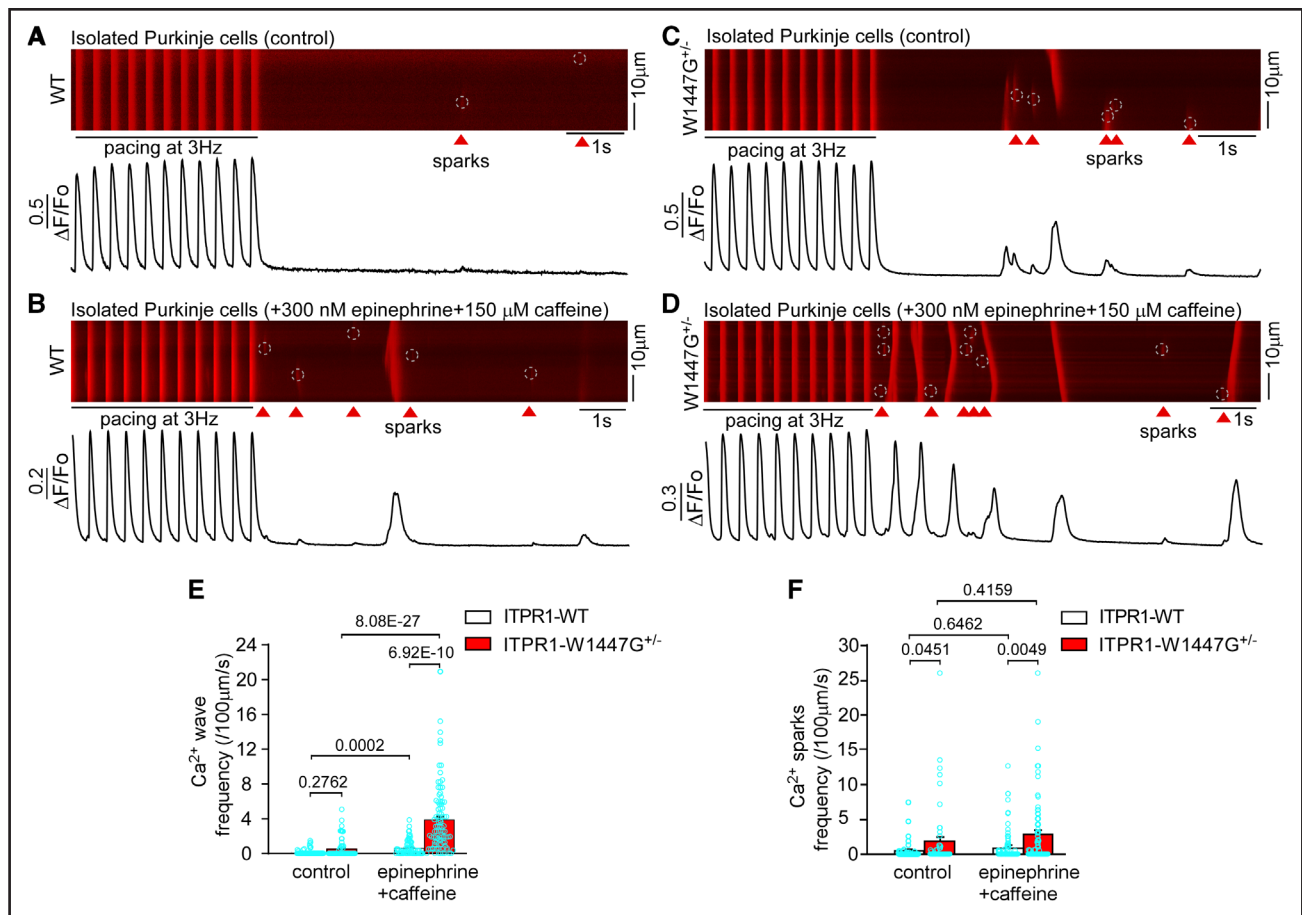


**Figure 5. The ITPR1-W1447G<sup>+/−</sup> GOF variant increases the propensity for spontaneous Ca<sup>2+</sup> release in isolated Purkinje cells.** Representative line-scan Ca<sup>2+</sup> images of isolated Cntn2-GFP-labeled ITPR1-WT Purkinje cells before (A) and after the treatment of 300 nM epinephrine plus 150 μM caffeine (B) or isolated Cntn2-GFP-labeled ITPR1-W1447G<sup>+/−</sup> Purkinje cells before (C) and after the treatment of 300 nM epinephrine plus 150 μM caffeine (D) during electrical field stimulation (3 Hz; indicated by a black line) and after the cessation of stimulation. The frequency of spontaneous Ca<sup>2+</sup> waves (E) and Ca<sup>2+</sup> sparks (F) in isolated Cntn2-GFP/ITPR1-WT and Cntn2-GFP/ITPR1-W1447G<sup>+/−</sup> Purkinje cells in the control condition or in the presence of epinephrine and caffeine. Red arrowheads and white dashed line circles indicate the occurrence of spontaneous Ca<sup>2+</sup> sparks. Data shown are mean ± SEM (for ITPR1-WT, n=73 Purkinje cells in the control condition, and n=70 cells in the presence of epinephrine and caffeine from 9 hearts; for ITPR1-W1447G<sup>+/−</sup>, n=66 Purkinje cells in the control condition and n=88 cells in the presence of epinephrine and caffeine from 9 hearts; Kruskal-Wallis test with Dunn post hoc test for obtaining the adjusted P values shown in E and F).

GOF enhances stress-induced, ryanodine-sensitive, spontaneous Ca<sup>2+</sup> release in isolated Purkinje cells.

We also assessed the effect of the ITPR1-W1447G<sup>+/−</sup> GOF variant on spontaneous Ca<sup>2+</sup> release upon addition of a membrane-permeable IP<sub>3</sub> ester (myo-inositol 1,4,5-trisphosphate hexakis [butyryloxymethyl], IP<sub>3</sub>BM) or a known IP<sub>3</sub>-generating hormone, ET-1 (endothelin-1), in isolated Cntn2-GFP/ITPR1-WT and Cntn2-GFP/ITPR1-W1447G<sup>+/−</sup> Purkinje cells. Both IP<sub>3</sub>BM and ET-1 increased Ca<sup>2+</sup> spark frequency in both Cntn2-GFP/ITPR1-WT and Cntn2-GFP/ITPR1-W1447G<sup>+/−</sup> GOF mutant Purkinje cells (Figures S9 and S10). The IP<sub>3</sub>BM- or ET-1-induced increase in Ca<sup>2+</sup> spark frequency in Cntn2-GFP/ITPR1-W1447G<sup>+/−</sup> GOF mutant Purkinje cells was significantly higher than that in Cntn2-GFP/ITPR1-WT cells (Figures S9 and S10). Furthermore, the frequency of IP<sub>3</sub>BM- or ET-1-induced Ca<sup>2+</sup> sparks were

markedly suppressed by a low concentration of ITPR inhibitor, 2-aminoethoxydiphenyl borate (2-APB) (2 μM; Figures S9 and S10), or were diminished by ryanodine (50 μM; Figure S11). These data indicate that the ITPR1-W1447G<sup>+/−</sup> GOF variant can also enhance the occurrence of IP<sub>3</sub>-induced Ca<sup>2+</sup> release that involves both the ITPRs and ryanodine receptors (RyRs). This is consistent with previous studies.<sup>23–25,28,56–59</sup>

It has previously been shown that ITPR1 is predominantly located at the cell periphery underneath the sarcolemma and the perinuclear region of Purkinje cells.<sup>23–25,28</sup> In line with this subcellular localization of ITPR1, IP<sub>3</sub>-induced Ca<sup>2+</sup> release events in Purkinje cells were primarily observed at the cell periphery and perinuclear region.<sup>23–25,28</sup> Consistent with those reported previously, we found that ITPR1 staining and IP<sub>3</sub>-induced Ca<sup>2+</sup> release events were predominantly located at the cell periphery and perinuclear



region of ITPR1-WT and ITPR1-W1447G<sup>+/-</sup> GOF mutant Purkinje cells with a similar pattern of subcellular distribution (Figures S12 and S13).

### ITPR1 GOF Increases Spontaneous Membrane Depolarizations in Purkinje Fibers but Not in Ventricular Myocytes in Heart Slices

Spontaneous intracellular Ca<sup>2+</sup> waves can alter membrane potentials in cardiac cells.<sup>32–36</sup> An important question is whether ITPR1 GOF-enhanced spontaneous Ca<sup>2+</sup> waves can evoke membrane depolarizations in Purkinje fibers. To this end, we performed confocal line-scanning membrane potential imaging of voltage-sensitive dye

(RH237)-loaded heart slices prepared from Cntn2-GFP-labeled ITPR1-WT, -W1447G<sup>+/-</sup>, and -D2594K<sup>+/-</sup> mice. No spontaneous membrane depolarizations were observed in Cntn2-GFP/ITPR1-WT or Cntn2-GFP/ITPR1-mutant Purkinje fibers or ventricular myocytes in the absence of epinephrine and caffeine (Figure S14). However, upon stimulation with epinephrine and caffeine, spontaneous membrane depolarizations were readily observed in Cntn2-GFP/ITPR1-W1447G<sup>+/-</sup> and Cntn2-GFP/ITPR1-D2594K<sup>+/-</sup> mutant Purkinje fibers, but not in Cntn2-GFP/ITPR1-WT Purkinje cells (Figure 6A, 6B, and 6D through 6F). In contrast, epinephrine and caffeine did not evoke spontaneous membrane depolarizations in ITPR1-WT, ITPR1-W1447G<sup>+/-</sup>, or ITPR1-D2594K<sup>+/-</sup>

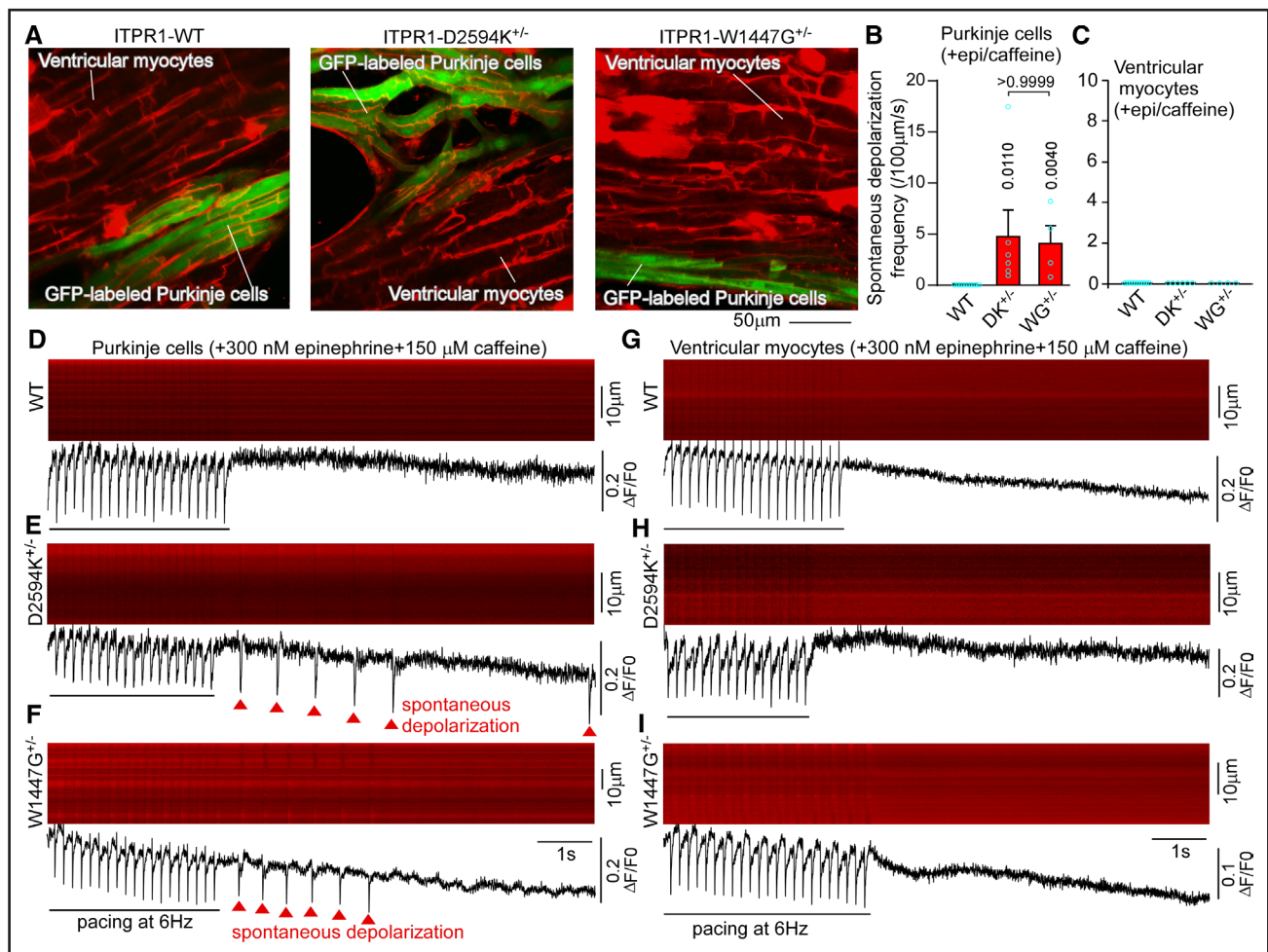


**Figure 6. ITPR1 GOF variants enhance spontaneous depolarizations in Purkinje cells but not in ventricular myocytes in heart slices.**

Confocal x-y images of Cntn2-GFP/ITPR1-WT (left), Cntn2-GFP/ITPR1-D2594K<sup>+/-</sup> (middle), and Cntn2-GFP/ITPR1-W1447G<sup>+/-</sup> (right) mouse heart slices loaded with RH237 voltage-sensing dye, showing the GFP-labeled Purkinje cells and RH237-loaded Purkinje cells and ventricular myocytes (A). Heart slices were perfused with 300 nM epinephrine plus 150 μM caffeine. The RH237 signals (membrane potential) in ITPR1-WT (D), ITPR1-D2594K<sup>+/-</sup> (E), and ITPR1-W1447G<sup>+/-</sup> (F) Cntn2-GFP-labeled Purkinje cells and in ITPR1-WT (G), ITPR1-D2594K<sup>+/-</sup> (H), and ITPR1-W1447G<sup>+/-</sup> (I) ventricular myocytes were recorded using line-scanning confocal imaging during electrical field stimulation (6 Hz; indicated by a black line) and after the cessation of stimulation. Frequency of spontaneous membrane depolarizations in ITPR1-WT, ITPR1-D2594K<sup>+/-</sup>, and ITPR1-W1447G<sup>+/-</sup> Cntn2-GFP-labeled Purkinje cells (B) and ventricular myocytes (C) in the presence of epinephrine and caffeine. The trace underneath each RH237 line-scan image represents the average intensity of the RH237 fluorescence signal along the entire scan-line. Data shown are mean±SEM (n=11 hearts for ITPR1-WT, 6 hearts for ITPR1-D2594K<sup>+/-</sup>, and 4 hearts for ITPR1-W1447G<sup>+/-</sup>; Kruskal-Wallis test with Dunn post hoc test for obtaining the adjusted *P* values shown in B and C).

ventricular myocytes devoid of neighboring Purkinje cells in heart slices (Figure 6C and 6G through 6I). Note that ventricular myocytes in intact hearts are coupled to Purkinje cells through the Purkinje-muscle junctions. However, in thin heart slices, some of these Purkinje-muscle junctions may have been removed, leading to patches of ventricular myocytes disconnected from Purkinje cells. The loss of this coupling between Purkinje cells and cardiomyocytes would prevent effective transmission of action potentials generated in Purkinje cells to the ventricular myocytes in thin heart slices. Taken together, these data indicate that ITPR1 GOF increases the propensity for stress-induced spontaneous membrane depolarizations in Purkinje fibers, but not in ventricular myocytes, which is again consistent with the low level of ITPR1 expression in ventricular myocytes.<sup>22–28</sup>

### ITPR1-W1447G<sup>+/-</sup> GOF Variant Increases the Propensity for Triggered Activity in Isolated Purkinje Cells

Spontaneous Ca<sup>2+</sup> waves can evoke DADs and triggered activity (ie, DAD-provoked action potentials) in Purkinje cells and consequently stress-induced VAs.<sup>32–36</sup> To determine whether spontaneous membrane depolarizations observed in Purkinje fibers resulted from DAD-provoked triggered activity, we performed whole cell current-clamp recordings of isolated Cntn2-GFP-labeled Purkinje cells. There was no significant difference in the frequency of DADs between Cntn2-GFP/ITPR1-W1447G<sup>+/-</sup> and Cntn2-GFP/ITPR1-WT Purkinje cells under the baseline condition (Figure 7A, 7C, and 7E). However, under stress condition, the frequency of DADs in Cntn2-GFP/W1447G<sup>+/-</sup> Purkinje cells was markedly increased compared with that in the Cntn2-GFP/ITPR1-WT Purkinje cells (Figure 7B, 7D, and 7E). Similarly, the frequency of triggered activity was not significantly different between Cntn2-GFP/ITPR1-W1447G<sup>+/-</sup> and Cntn2-GFP/ITPR1-WT Purkinje cells under baseline conditions (Figure 7A, 7C, and 7F), but it was markedly enhanced in Cntn2-GFP/ITPR1-W1447G<sup>+/-</sup> Purkinje cells under stress conditions (Figure 7B, 7D, and 7F). The ITPR1-W1447G<sup>+/-</sup> mutation also significantly increased the fraction of Cntn2-GFP-labeled Purkinje cells that displayed triggered activities under both baseline and stress conditions (Figure 7G). Collectively, these data suggest that ITPR1 GOF predisposes to stress-induced VAs by increasing the propensity for spontaneous Ca<sup>2+</sup> waves, DADs, and triggered activities in Purkinje cells.

### Human ITPR1 GOF Variants Are Associated With Increased Risk for Cardiac Arrhythmias

Our animal studies demonstrate that ITPR1 GOF increases the susceptibility to cardiac arrhythmias in mice. This raises an important question of whether ITPR1

GOF is also associated with increased risk for cardiac arrhythmias in humans. To this end, we analyzed the exome sequence data for 10% of the cohort (referred to as 50 000 UK Biobank participants exome data set) released by the UK Biobank,<sup>60</sup> a large-scale biomedical database and research resource containing genotypes and health information from half a million United Kingdom participants.<sup>61</sup> It is interesting that, among the 33 human ITPR1 missense variants we have functionally characterized (Figure 1; Table S1), 3 variants were also in the 50 000 UK Biobank participants exome data set: 2 weak GOF variants (D1154G and T1474I, also present on the Affymetrix array and therefore genotyped in the full UK Biobank data set) and one moderate GOF variant (E1490K). None of the strong GOF variants we have functionally characterized were present in the 50 000 UK Biobank participants exome data set. A question arises: Are these moderate and weak ITPR1 GOF variants associated with increased risk for cardiac arrhythmias? It is interesting that there are 2 carriers of the moderate GOF ITPR1-E1490K variant within the 50 000 UK Biobank participants exome data set, one of which was diagnosed with atrial fibrillation and flutter. The clinical diagnoses of the other E1490K carrier were unremarkable. For the weak ITPR1 GOF variants (D1154G and T1474I), there are 854 and 680 carriers, respectively, among the UK Biobank participants with white British ancestry. Our genetic analysis (adjusted for age and sex) showed that carriers of the ITPR1-D1154G variant had a nominally significantly increased risk for tachycardia (*International Classification of Diseases, 10th Revision*, R00.0) with an odds ratio of 1.97 ( $P=3.6\times 10^{-2}$ ). For the ITPR1-T1474I variant, no association was observed.

Because rare variants are notoriously difficult to link to phenotypes in association studies (because of low statistical power), a gene-based burden analysis combining all rare coding variants into a single test has been performed by Lee et al for 791 phenotypes, and the results were made available through a browser (<http://ukb-50kexome.leelabs.org/gene/ITPR1>). ITPR1 was found to be associated with the following partially overlapping phenotype codes: paroxysmal tachycardia (427.1; overall  $P=2.4\times 10^{-4}$ ), paroxysmal supraventricular tachycardia (427.11; overall  $P=1.6\times 10^{-3}$ ), and cardiac arrest and ventricular fibrillation (427.4; overall  $P=0.014$ ; Table S3). These associations were driven by missense variants and not by stop-gain or frame-shift variants. To assess the potential association between ITPR1 GOF and increased risk for arrhythmias, we selected top ITPR1 variants identified in each of these diagnoses, which are highly conserved in all 3 ITPR1 isoforms across different species. These include ITPR1 variants V802M, V1353L, I1297M, H1421Q, K2134Q, P2747S, and I1297V. We then generated HEK293 cell lines expressing each of these variants and determined the EC<sub>50</sub> of each variant to IP<sub>3</sub> activation using the IP<sub>3</sub>-induced Ca<sup>2+</sup> release assay

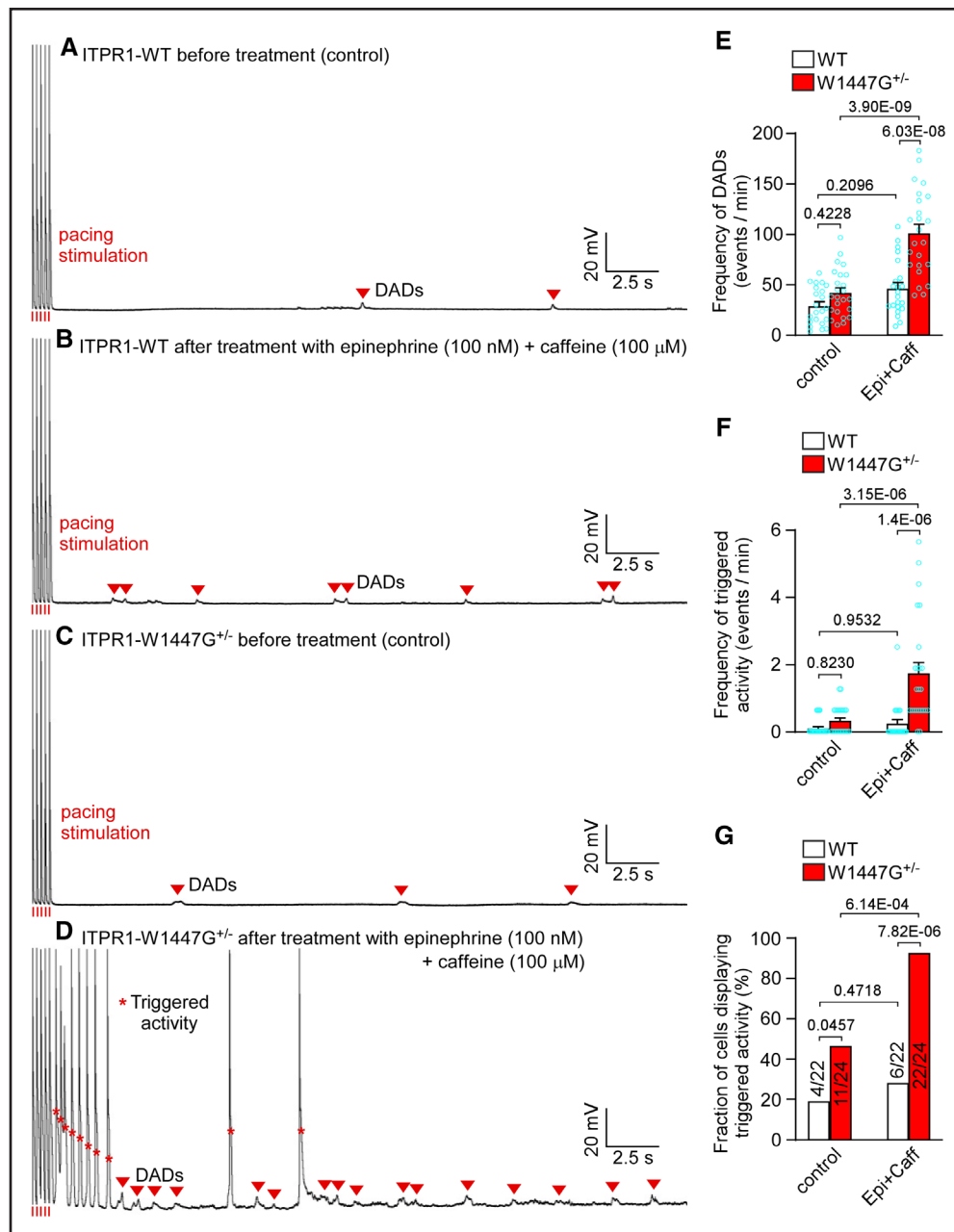


**Figure 7. The ITPR1-W1447G<sup>+/-</sup> GOF variant enhances triggered activity in isolated Purkinje cells.**

Membrane potentials in Cntn2-GFP/ITPR1-WT Purkinje cells before (A) and after the treatment of epinephrine and caffeine (B) or in Cntn2-GFP/ITPR1-W1447G<sup>+/-</sup> Purkinje cells before (C) and after the treatment of epinephrine and caffeine (D) were recorded using whole cell patch-clamp recordings in the current clamp mode. E, The frequency of delayed afterdepolarizations (DADs), (F) the frequency of triggered activity, and (G) the fraction of cells displaying triggered activity in Cntn2-GFP/ITPR1-WT and Cntn2-GFP/ITPR1-W1447G<sup>+/-</sup> Purkinje cells before (control) and after epinephrine and caffeine treatment. Red arrowheads indicate the presence of DADs, red asterisks triggered activity, and red vertical bars pacing stimulations. Data shown are mean±SEM (n=22 cells from 7 ITPR1-WT hearts, n=24 cells from 8 ITPR1-W1447G<sup>+/-</sup> hearts; 2-way ANOVA with Tukey post hoc test was performed for obtaining *P* values shown in E and F and  $\chi^2$  test for determining *P* values shown in G).

in HEK293 cells. Remarkably, we found that all these 7 ITPR1 variants exhibited significantly increased sensitivity to IP<sub>3</sub> activation (ie, GOF; Figure 8). The GOF phenotype of ITPR1 variants, ITPR1-V802M, -I1297M, and -I1297V, were confirmed using the HEK-3KO cells in which all 3 ITPR isoforms have been knocked out (Figure S2). These data are consistent with the notion that ITPR1 GOF increases the risk for cardiac arrhythmias in humans.

## DISCUSSION

Despite its widespread tissue expression, mutations in the *ITPR1* gene have primarily been linked to movement disorders.<sup>9–11,42,43</sup> The pathological ramifications of ITPR1 dysfunction in nonneuronal tissues are poorly understood. For instance, ITPR1 is expressed in cardiac Purkinje fibers and has been implicated in cardiac arrhythmias,<sup>22–28</sup>

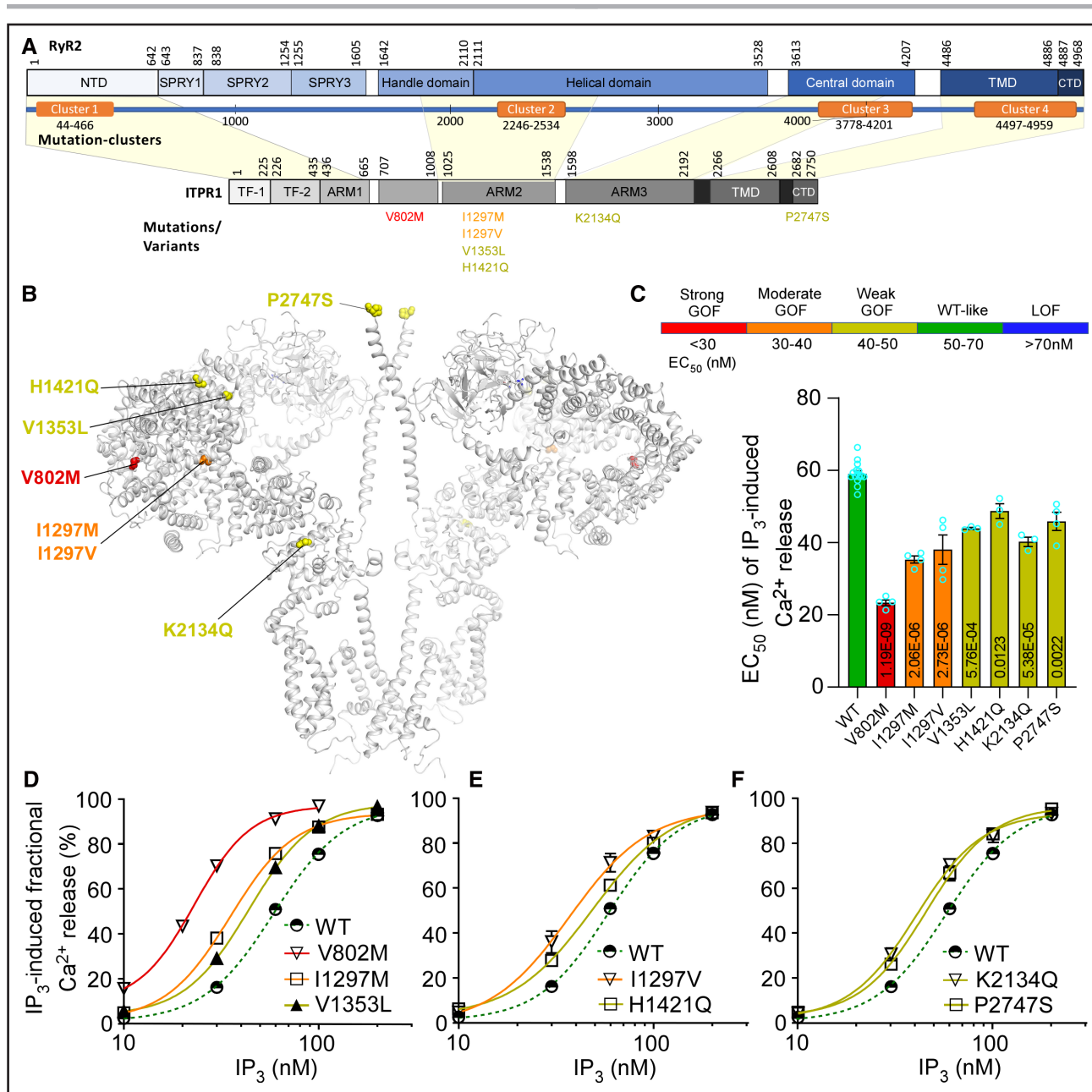


**Figure 8. Human ITPR1 variants associated with increased risk for cardiac arrhythmias increase the sensitivity of ITPR1 to activation by IP<sub>3</sub>.**

**A**, A schematic diagram of the linear sequences of RyR2 and ITPR1. Major domains of RyR2 are shown as solid blue boxes. The orange boxes indicate 4 disease-associated variant clusters (hotspots) of RyR2. Major domains of ITPR1 are shown as solid gray/black boxes. The corresponding homologous regions of ITPR1 and RyR2 are indicated by yellow-shaded areas. Human ITPR1 variants characterized are grouped under domains they reside in and are color-coded as those shown in **C**. **B**, Locations of ITPR1 variants in the 3-dimensional structure of ITPR1 (PDB: 6MU2). **C**, EC<sub>50</sub> values of IP<sub>3</sub> induced Ca<sup>2+</sup> release in HEK293 cells expressing ITPR1 WT or variants with the range of EC<sub>50</sub> values color-coded. Data shown are mean±SEM (n=3 or 4; 1-way ANOVA with Dunnett post hoc test for obtaining *P* values shown in **C**). **D** through **F**, The dose-response curves of IP<sub>3</sub>-induced fractional Ca<sup>2+</sup> release in HEK293 cells expressing ITPR1 WT, V802M, I1297M, and V1353L (**D**), I1297V and H1421Q (**E**), and K2134Q and P2747S (**F**) were determined by measuring the signal drop in ER Ca<sup>2+</sup> level after a given IP<sub>3</sub> dose and normalized to the total ER Ca<sup>2+</sup> store (the drop in ER Ca<sup>2+</sup> level after addition of 1 μM IP<sub>3</sub> plus 4 μM CPA). Data shown are mean±SEM (n=3 or 4). GOF indicates gain-of-function; and LOF, loss-of-function.

but direct evidence for the role of ITPR1 in Purkinje-related arrhythmias has yet to be demonstrated. It is interesting that nearly all disease-linked ITPR1 variants characterized to date are loss-of-function,<sup>9–11,42,43</sup> leav-

ing the pathological significance of ITPR1 GOF largely unknown. Here, we used ITPR1 mutant mouse models to assess the role of enhanced ITPR1 function in cardiac arrhythmias. We performed confocal in situ Ca<sup>2+</sup> and



voltage imaging on Purkinje fibers in heart slices and  $\text{Ca}^{2+}$  imaging and patch-clamp recordings on isolated Purkinje cells. We revealed, for the first time, that ITPR1 GOF variants enhanced the propensity for spontaneous  $\text{Ca}^{2+}$  waves, DADs, and triggered activity in Purkinje cells, and increased the susceptibility to stress-induced VAs in mice. Given that  $\text{Ca}^{2+}$  mishandling in Purkinje cells is a major source of cardiac arrhythmia,<sup>23,29,30,62,63</sup> our findings suggest that ITPR1 is a potential risk gene for cardiac arrhythmias.

An important question is whether ITPR1 GOF also increases cardiac arrhythmia risk in humans. To address this, we first determined whether ITPR1 GOF variants exist in humans. We performed a systematic in vitro functional characterization of a large number of known human ITPR1 variants and identified 28 GOF variants. Unfortunately, information about arrhythmia susceptibility of these human ITPR1 GOF variants is not available, and there is no access to these ITPR1 GOF variant carriers for further clinical evaluations. Hence, the arrhythmia susceptibility of these human ITPR1 GOF variant carriers remains to be investigated. Recently, Lee et al exploited the UK Biobank exome data set and conducted gene-based burden testing (or gene-based collapsing analysis) to identify potential associations of genes with rare disorders (<http://ukb-50kexome.leelabsg.org>). Lee et al (<http://ukb-50kexome.leelabsg.org/gene/ITPR1>) reported that there are potential associations of rare ITPR1 missense (but not stop-gain or frame-shift) variants with cardiovascular events, including paroxysmal tachycardia (overall  $P=2.4 \times 10^{-4}$ ), paroxysmal supraventricular tachycardia (overall  $P=1.6 \times 10^{-3}$ ), and cardiac arrest and ventricular fibrillation (overall  $P=0.014$ ; Table S3). We performed in vitro functional characterization of those ITPR1 rare variants that are most highly associated with one or more of these diagnoses and that are conserved in all 3 ITPR1 isotypes (Table S3). Remarkably, all ITPR1 rare variants characterized, including V802M, V1353L, I1297M, H1421Q, K2134Q, P2747S, and I1297V, are GOF. Therefore, these findings are consistent with the predisposition of ITPR1 GOF variants to increased risk for cardiac arrhythmias in humans. It is, however, important to note that the gene-based collapsing analyses performed and reported by Lee et al are based on small number of carriers and only show potential association of ITPR1 GOF variants with increased risk for cardiac arrhythmias with certain probabilities (overall  $P$  values) in humans, which is consistent with our observations in mice. To definitively establish the association between ITPR1 GOF and cardiac arrhythmias, large case and control samples (not population-based samples) that have undergone sequencing or identification and characterization of a large pedigree where an ITPR1 GOF variant is segregating with the cardiac arrhythmia phenotype in multiple generations would be required. Cur-

rently, the *ITPR1* gene is included in the gene panel for clinical genetic testing of ataxia. Including the *ITPR1* gene in the gene panel for clinical genetic testing of cardiac arrhythmias would help to determine the role of ITPR1 in cardiac arrhythmias.

Cardiac Purkinje cells express both the ITPR1 that is located beneath the sarcolemma and the RyR2 that is located predominantly in the interior of the cell.<sup>23–25,28,56</sup> It is believed that local  $\text{Ca}^{2+}$  release by ITPR1 serves as an initiator of a larger  $\text{Ca}^{2+}$  release from RyR2 that leads to propagating  $\text{Ca}^{2+}$  waves.<sup>23–25,28,56</sup> Physical and emotional stresses can activate the  $\beta$ -adrenergic receptor–cAMP–PKA (protein kinase A) signaling pathway that enhances RyR2 mediated  $\text{Ca}^{2+}$  release in Purkinje cells. These stresses can also activate the  $\alpha$ -adrenergic receptor–PLC (phospholipase C)– $\text{IP}_3$  signaling pathway that increases ITPR1-mediated  $\text{Ca}^{2+}$  release in the same cells.<sup>29,30,36,63–67</sup> Thus, enhanced ITPR1 and RyR2 function may synergistically promote the initiation of local spontaneous  $\text{Ca}^{2+}$  release and the generation/propagation of arrhythmogenic  $\text{Ca}^{2+}$  waves in Purkinje cells. This in turn would increase the propensity for triggered activity. Consistent with this view, we found that pretreatment with ryanodine completely abolished epinephrine/cafeine-induced  $\text{Ca}^{2+}$  waves and  $\text{Ca}^{2+}$  sparks in ITPR1-W1447G<sup>+/-</sup> GOF mutant Purkinje cells. This dual ITPR1- and RyR2-controlled  $\text{Ca}^{2+}$  release mechanism may make the Purkinje cells highly vulnerable to stress-induced  $\text{Ca}^{2+}$  dysregulation and  $\text{Ca}^{2+}$ -triggered VAs. This vulnerability of Purkinje cells to  $\text{Ca}^{2+}$  dysregulation highlights the importance of targeting both the  $\beta$ - and  $\alpha$ -adrenergic receptors as well as both the RyR2- and ITPR1-mediated abnormal  $\text{Ca}^{2+}$  release for suppressing stress-induced VAs.

$\text{Ca}^{2+}$  handling in Purkinje cells is often studied at the level of isolated cells.<sup>51–53</sup> Our present work demonstrated the feasibility of studying  $\text{Ca}^{2+}$  handling in Purkinje cells in situ in heart slices. We used the Cntn2-GFP mice in which Purkinje cells are fluorescently labeled. Line-scanning confocal imaging was used to assess  $\text{Ca}^{2+}$  dynamics in individual Purkinje cells and ventricular myocytes within these heart slices. It is interesting that there were few or no spontaneous  $\text{Ca}^{2+}$  release events in Purkinje cells or ventricular myocytes in heart slices prepared from WT mice under either rest or stimulating conditions. In contrast, spontaneous  $\text{Ca}^{2+}$  release events were readily observed in Purkinje cells, but not in ventricular myocytes, in heart slices from ITPR1-W1447G<sup>+/-</sup> or -D2594K<sup>+/-</sup> GOF mutant mice under both the rest and stimulating conditions. We also performed membrane voltage imaging of Purkinje cells and ventricular myocytes in situ in heart slices and demonstrated that pharmacological stress (epinephrine and caffeine) only evoked membrane depolarizations in Purkinje cells, but not in ventricular myocytes, in the ITPR1-W1447G<sup>+/-</sup> or -D2594K<sup>+/-</sup> GOF mutant heart slices. Thus, this heart

slice preparation represents a reliable approach to studying  $\text{Ca}^{2+}$  handling in Purkinje cells.

The ITPR1-D2594K<sup>+/−</sup> GOF mutation enhanced ITPR1 activation at low  $\text{Ca}^{2+}$  levels and suppressed  $\text{Ca}^{2+}$ -dependent inhibition at high levels.<sup>68</sup> However, the effects of other ITPR1 GOF mutations on the  $\text{Ca}^{2+}$  and  $\text{IP}_3$  dependence of channel activation remain unexplored. Future studies on the mechanisms by which ITPR1 GOF affects channel function are needed.

In summary, the present study identified many novel human ITPR1 GOF variants and generated the first mouse model of human ITPR1 hyperactivity. We showed, for the first time, that ITPR1 GOF enhances spontaneous  $\text{Ca}^{2+}$  release and triggered activity in Purkinje cells and arrhythmia susceptibility in mice. Furthermore, gene-based collapsing analysis suggests that ITPR1 GOF also increases the risk for cardiac arrhythmias in humans. Given that ITPR1 is expressed in a variety of cells and tissues, our novel ITPR1 GOF mutant mouse models may provide the much-needed tool for investigating the significance of ITPR1 hyperactivity in a wide range of disorders.

## ARTICLE INFORMATION

Received May 21, 2024; accepted October 30, 2024.

### Affiliations

Department of Physiology and Pharmacology, Libin Cardiovascular Institute, University of Calgary, Canada (B.S., M. Ni, Y.L., Z.S., H.W., H.-L.Z., J.W., D.B., S.C., W.G., J.Y., S.T., J.P.E., R.W., S.R.W.C.). Medical School, Kunming University of Science and Technology, China (B.S.). Department of Internal Medicine, Institute of Hypertension, Tongji Hospital, Tongji Medical College, Huazhong University of Science and Technology, Wuhan, China (Y.L.). Department of Chemistry and Bioscience (M.T.S., M.B., P.D.R.), Department of Health Science and Technology (M. Nyegaard), Aalborg University, Denmark. Department of Medicine, University of California at San Diego, La Jolla (Y.M., J.C.). Department of Automatic Control, Universitat Politècnica de Catalunya, Barcelona, Spain (A.V., R.B.). Biomedical Research Institute Barcelona (IIBB)-Spanish National Research Council (CSIC) and Sant Pau Biomedical Research Institute (IIB Sant Pau), Hospital de Sant Pau, Barcelona, Spain (L.H.-M.). Leon H. Charney Division of Cardiology, New York University Langone Health, New York, NY (G.I.F.). Division of Cardiology, Department of Pediatrics, University of British Columbia, Vancouver, Canada (S.S.). Department of Clinical and Experimental Cardiology, Heart Center, Amsterdam University Medical Centre, Academic Medical Center Location, The Netherlands (A.A.M.W.). European Reference Network "ERN GUARD-heart", Amsterdam, The Netherlands (A.A.M.W.). Department of Physiology and Biophysics, Rush University Medical Center, Chicago, IL (M.F., J.R.-F., S.R.W.C.). Department of Biomedicine, Aarhus University, Denmark (M. Nyegaard).

### Acknowledgments

B.S., M.Ni, Y.L., Z.S., H.W., H.-L.Z., J.W., D.B., R.W., A.V., R.B., L.H.-M., M.T.O., J.C., M.F., J.R.-F., M.Nyegaard, and S.R.W.C. designed the research; B.S., M.Ni, Y.L., Z.S., H.W., H.-L.Z., J.W., D.B., S.C., W.G., J.Y., S.T., J.P.E., R.W., Y.M., and A.V. performed the research; B.S., M.Ni, Y.L., Z.S., H.W., J.W., D.B., S.C., W.G., M.S., M.B., A.V., R.B., and S.R.W.C. analyzed data; P.D.R. and M.Nyegaard performed human genetic association analyses; M.T.O., G.I.F., J.C., S.S., A.A.M.W., M.F., J.R.-F., M.Nyegaard, and S.R.W.C. provided reagents or research support; and B.S., M.Ni, Y.L., Z.S., J.W., D.B., R.W., P.D.R., S.S., A.A.M.W., M.F., J.R.-F., M.Nyegaard, and S.R.W.C. wrote the article.

### Sources of Funding

This work was supported by research grants from the Canadian Institutes of Health Research (PJT-173352) to S.R.W.C.; the Heart and Stroke Foundation of Canada (G-22-0032243) to S.R.W.C.; the National Natural Science Foundation of China (82373872 and 81903611) to B.S.; the E-Rare Joint Transnational Call for Proposals 2015 "Improving Diagnosis and Treatment of Catecholaminergic Polymorphic Ventricular Tachycardia: Integrating Clinical and Basic Science" to

S.R.W.C., S.S., and A.A.M.W.; CVON-PREDICT2 to A.A.M.W.; the National Institutes of Health (R01HL057832) to S.R.W.C. and M.F.; R01GM111397 to S.R.W.C., M.F., and J.R.-F.; National Institutes of Health grant No. HL105983 to G.I.F., the Spanish Ministry of Science Innovation and Universities SAF2017-88019-C3-1R and 2R to L.H.-M. and R.B.; Marato-TV3 20152030 to L.H.-M.; and Generalitat de Catalunya SGR2017-1769 to L.H.-M. S.R.W.C. holds the Heart and Stroke Foundation chair in cardiovascular research (END611955). The human phenotypic and genetic data were obtained from the UK Biobank under application ID 60032. B.S. and J.Y. are recipients of the Alberta Innovates-Health Solutions fellowship award. Z.S. is a recipient of the University of Calgary Eyes High Postdoctoral fellowship award. H.W. and J.W. are recipients of the Libin Cardiovascular Institute and Cumming School of Medicine postdoctoral fellowship award. W.G. is a recipient of the Alberta Innovates-Health Solutions studentship award. S.T. is a recipient of the Libin Cardiovascular Institute graduate studentship award.

### Disclosures

None.

### Supplemental Material

Supplemental Methods  
Tables S1–S3  
Figure S1–S14  
References 69–91

## REFERENCES

- Patel S, Joseph SK, Thomas AP. Molecular properties of inositol 1,4,5-trisphosphate receptors. *Cell Calcium*. 1999;25:247–264. doi: 10.1054/ceca.1999.0021
- Stathopoulos PB, Seo MD, Enomoto M, Amador FJ, Ishiyama N, Ikura M. Themes and variations in ER/SR calcium release channels: structure and function. *Physiology (Bethesda)*. 2012;27:331–342. doi: 10.1152/physiol.00013.2012
- Parys JB, De Smedt H. Inositol 1,4,5-trisphosphate and its receptors. *Adv Exp Med Biol*. 2012;740:255–279. doi: 10.1007/978-94-007-2888-2\_11
- Berridge MJ. The inositol trisphosphate/calcium signaling pathway in health and disease. *Physiol Rev*. 2016;96:1261–1296. doi: 10.1152/physrev.00006.2016
- Berridge MJ. Inositol trisphosphate and calcium signalling mechanisms. *Biochim Biophys Acta*. 2009;1793:933–940. doi: 10.1016/j.bbamcr.2008.10.005
- Foskett JK, White C, Cheung KH, Mak DO. Inositol trisphosphate receptor  $\text{Ca}^{2+}$  release channels. *Physiol Rev*. 2007;87:593–658. doi: 10.1152/physrev.00035.2006
- Varga-Szabo D, Braun A, Nieswandt B. Calcium signaling in platelets. *J Thromb Haemost*. 2009;7:1057–1066. doi: 10.1111/j.1538-7836.2009.03455.x
- Decuyper JP, Monaco G, Bultynck G, Missiaen L, De Smedt H, Parys JB. The IP(3) receptor-mitochondria connection in apoptosis and autophagy. *Biochim Biophys Acta*. 2011;1813:1003–1013. doi: 10.1016/j.bbamcr.2010.11.023
- Hisatsune C, Mikoshiba K. IP(3) receptor mutations and brain diseases in human and rodents. *J Neurochem*. 2017;141:790–807. doi: 10.1111/jnc.13991
- Terry LE, Alzayady KJ, Furati E, Yule DI. Inositol 1,4,5-trisphosphate receptor mutations associated with human disease. *Messenger (Los Angel)*. 2018;6:29–44.
- Kerkhofs M, Seitaj B, Ivanova H, Monaco G, Bultynck G, Parys JB. Pathophysiological consequences of isoform-specific IP3 receptor mutations. *Biochim Biophys Acta Mol Cell Res*. 2018;1865:1707–1717. doi: 10.1016/j.bbamcr.2018.06.004
- Furuichi T, Mikoshiba K. Inositol 1, 4, 5-trisphosphate receptor-mediated  $\text{Ca}^{2+}$  signaling in the brain. *J Neurochem*. 1995;64:953–960. doi: 10.1046/j.1471-4159.1995.64030953.x
- Dent MA, Raisman G, Lai FA. Expression of type 1 inositol 1,4,5-trisphosphate receptor during axogenesis and synaptic contact in the central and peripheral nervous system of developing rat. *Development*. 1996;122:1029–1039. doi: 10.1242/dev.122.3.1029
- Matsumoto M, Nakagawa T, Inoue T, Nagata E, Tanaka K, Takano H, Minowa O, Kuno J, Sakakibara S, Yamada M, et al. Ataxia and epileptic seizures in mice lacking type 1 inositol 1,4,5-trisphosphate receptor. *Nature*. 1996;379:168–171. doi: 10.1038/379168a0
- Furuichi T, Yoshikawa S, Miyawaki A, Wada K, Maeda N, Mikoshiba K. Primary structure and functional expression of the inositol 1,4,5- trisphosphate-binding protein P400. *Nature*. 1989;342:32–38. doi: 10.1038/342032a0

16. Goto J, Mikoshiba K. Inositol 1,4,5-trisphosphate receptor-mediated calcium release in Purkinje cells: from molecular mechanism to behavior. *Cerebellum*. 2011;10:820–833. doi: 10.1007/s12311-011-0270-5
17. Wang TL, Sterling P, Vardi N. Localization of type I inositol 1,4,5-trisphosphate receptor in the outer segments of mammalian cones. *J Neurosci*. 1999;19:4221–4228. doi: 10.1523/JNEUROSCI.19-11-04221.1999
18. Walensky LD, Snyder SH. Inositol 1,4,5-trisphosphate receptors selectively localized to the acrosomes of mammalian sperm. *J Cell Biol*. 1995;130:857–869. doi: 10.1083/jcb.130.4.857
19. Goud PT, Goud AP, Leybaert L, Van Oostveldt P, Mikoshiba K, Diamond MP, Dhont M. Inositol 1,4,5-trisphosphate receptor function in human oocytes: calcium responses and oocyte activation-related phenomena induced by photolytic release of InsP(3) are blocked by a specific antibody to the type I receptor. *Mol Hum Reprod*. 2002;8:912–918. doi: 10.1093/molehr/8.10.912
20. Wang Y, Chen J, Wang Y, Taylor CW, Hirata Y, Hagiwara H, Mikoshiba K, Toyo-oka T, Omata M, Sakaki Y. Crucial role of type 1, but not type 3, inositol 1,4,5-trisphosphate (IP(3)) receptors in IP(3)-induced Ca(2+) release, capacitative Ca(2+) entry, and proliferation of A7r5 vascular smooth muscle cells. *Circ Res*. 2001;88:202–209. doi: 10.1161/01.res.88.2.202
21. Smutzer G, Zimmerman JE, Han LY, Ruschinsky DD, Arnold SE, Yu X, Kratskin I. Inositol 1,4,5-trisphosphate receptor expression in odontoblast cells. *Biochim Biophys Acta*. 1997;1358:221–228. doi: 10.1016/s0167-4889(97)00075-x
22. Gorza L, Schiaffino S, Volpe P. Inositol 1,4,5-trisphosphate receptor in heart: evidence for its concentration in Purkinje myocytes of the conduction system. *J Cell Biol*. 1993;121:345–353. doi: 10.1083/jcb.121.2.345
23. Stuyvers BD, Dun W, Matkovich S, Sorrentino V, Boyden PA, ter Keurs HE. Ca2+ sparks and waves in canine Purkinje cells: a triple layered system of Ca2+ activation. *Circ Res*. 2005;97:35–43. doi: 10.1161/01.RES.0000173375.26489.fe
24. Ter Keurs HE, Boyden PA. Calcium and arrhythmogenesis. *Physiol Rev*. 2007;87:457–506. doi: 10.1152/physrev.00011.2006
25. Hirose M, Stuyvers B, Dun W, Ter Keurs H, Boyden PA. Wide long lasting perinuclear Ca2+ release events generated by an interaction between ryanodine and IP3 receptors in canine Purkinje cells. *J Mol Cell Cardiol*. 2008;45:176–184. doi: 10.1016/j.jymcc.2008.05.008
26. Bootman MD, Roderick HL. Why, where, and when do cardiac myocytes express inositol 1,4,5-trisphosphate receptors? *Am J Physiol Heart Circ Physiol*. 2008;294:H579–H581. doi: 10.1152/ajpheart.01378.2007
27. Ju YK, Woodcock EA, Allen DG, Cannell MB. Inositol 1,4,5-trisphosphate receptors and pacemaker rhythms. *J Mol Cell Cardiol*. 2012;53:375–381. doi: 10.1016/j.jymcc.2012.06.004
28. Daniels RE, Haq KT, Miller LS, Chia EW, Miura M, Sorrentino V, McGuire JJ, Stuyvers BD. Cardiac expression of ryanodine receptor subtype 3; a strategic component in the intracellular Ca(2+) release system of Purkinje fibers in large mammalian heart. *J Mol Cell Cardiol*. 2017;104:31–42. doi: 10.1016/j.jymcc.2017.01.011
29. Boyden PA. Purkinje physiology and pathophysiology. *J Interv Cardiac Electrophysiol*. 2018;52:255–262. doi: 10.1007/s10840-018-0414-3
30. Wilde AAM, Garan H, Boyden PA. Role of the Purkinje system in heritable arrhythmias. *Heart Rhythm*. 2019;16:1121–1126. doi: 10.1016/j.hrthm.2019.01.034
31. Priori SG, Corr PB. Mechanisms underlying early and delayed afterdepolarizations induced by catecholamines. *Am J Physiol*. 1990;258:H1796–H1805. doi: 10.1152/ajpheart.1990.258.6.H1796
32. Lakatta EG, Guarnieri T. Spontaneous myocardial calcium oscillations: are they linked to ventricular fibrillation? *J Cardiovasc Electrophysiol*. 1993;4:473–489. doi: 10.1111/j.1540-8167.1993.tb01285.x
33. Schlotthauer K, Bers DM. Sarcoplasmic reticulum Ca(2+) release causes myocyte depolarization. Underlying mechanism and threshold for triggered action potentials. *Circ Res*. 2000;87:774–780. doi: 10.1161/01.res.87.9.774
34. Bers DM. Calcium and cardiac rhythms: physiological and pathophysiological. *Circ Res*. 2002;90:14–17.
35. Pogwizd SM, Bers DM. Cellular basis of triggered arrhythmias in heart failure. *Trends Cardiovasc Med*. 2004;14:61–66. doi: 10.1016/j.tcm.2003.12.002
36. Priori SG, Chen SR. Inherited dysfunction of sarcoplasmic reticulum Ca2+ handling and arrhythmogenesis. *Circ Res*. 2011;108:871–883. doi: 10.1161/CIRCRESAHA.110.226845
37. Napolitano C, Priori SG. Diagnosis and treatment of catecholaminergic polymorphic ventricular tachycardia. *Heart Rhythm*. 2007;4:675–678. doi: 10.1016/j.hrthm.2006.12.048
38. Medeiros-Domingo A, Bhuiyan ZA, Tester DJ, Hofman N, Bikker H, van Tintelen JP, Manners MM, Wilde AA, Ackerman MJ. The RYR2-encoded ryanodine receptor/calcium release channel in patients diagnosed previously with either catecholaminergic polymorphic ventricular tachycardia or genotype negative, exercise-induced long QT syndrome: a comprehensive open reading frame mutational analysis. *J Am Coll Cardiol*. 2009;54:2065–2074. doi: 10.1016/j.jacc.2009.08.022
39. Lieve KV, van der Werf C, Wilde AA. Catecholaminergic polymorphic ventricular tachycardia. *Circ J*. 2016;80:1285–1291. doi: 10.1253/circj.CJ-16-0326
40. Garcia ML, Boehning D. Cardiac inositol 1,4,5-trisphosphate receptors. *Biochim Biophys Acta Mol Cell Res*. 2017;1864:907–914. doi: 10.1016/j.bbamcr.2016.11.017
41. Sun B, Ni M, Tian S, Guo W, Cai S, Sondergaard MT, Chen Y, Mu Y, Estillore JP, Wang R, et al. A gain-of-function mutation in the ITPR1 gating domain causes male infertility in mice. *J Cell Physiol*. 2022;237:3305–3316. doi: 10.1002/jcp.30783
42. Foskett JK. Inositol trisphosphate receptor Ca2+ release channels in neurological diseases. *Pflügers Arch*. 2010;460:481–494. doi: 10.1007/s00424-010-0826-0
43. Bezprozvanny I. Role of inositol 1,4,5-trisphosphate receptors in pathogenesis of Huntington's disease and spinocerebellar ataxias. *Neurochem Res*. 2011;36:1186–1197. doi: 10.1007/s11064-010-0393-y
44. Cerrone M, Colombi B, Santoro M, di Barletta MR, Scelsi M, Villani L, Napolitano C, Priori SG. Bidirectional ventricular tachycardia and fibrillation elicited in a knock-in mouse model carrier of a mutation in the cardiac ryanodine receptor. *Circ Res*. 2005;96:e77–e82. doi: 10.1161/01.RES.0000169067.51055.72
45. Zhou Q, Xiao J, Jiang D, Wang R, Vembaiyan K, Wang A, Smith CD, Xie C, Chen W, Zhang J, et al. Carvedilol and its new analogs suppress arrhythmogenic store overload-induced Ca2+ release. *Nat Med*. 2011;17:1003–1009. doi: 10.1038/nm.2406
46. Chen B, Guo A, Gao Z, Wei S, Xie YP, Chen SR, Anderson ME, Song LS. In situ confocal imaging in intact heart reveals stress-induced Ca(2+) release variability in a murine catecholaminergic polymorphic ventricular tachycardia model of type 2 ryanodine receptor(R4496C/+) mutation. *Circ Arrhythm Electrophysiol*. 2012;5:841–849. doi: 10.1161/CIRCEP.111.969733
47. Zhang J, Zhou Q, Smith CD, Chen H, Tan Z, Chen B, Nani A, Wu G, Song LS, Fill M, et al. Non-beta-blocking R-carvedilol enantiomer suppresses Ca2+ waves and stress-induced ventricular tachyarrhythmia without lowering heart rate or blood pressure. *Biochem J*. 2015;470:233–242. doi: 10.1042/BJ20150548
48. Loza R, Benkusky NA, Powers PP, Hacker T, Noujaim S, Ackerman MJ, Jalife J, Valdivia HH. Heterogeneity of ryanodine receptor dysfunction in a mouse model of catecholaminergic polymorphic ventricular tachycardia. *Circ Res*. 2013;112:298–308. doi: 10.1161/CIRCRESAHA.112.274803
49. Chen X, Weber C, Farrell ET, Alvarado FJ, Zhao YT, Gómez AM, Valdivia HH. Sorcin ablation plus  $\beta$ -adrenergic stimulation generate an arrhythmogenic substrate in mouse ventricular myocytes. *J Mol Cell Cardiol*. 2018;114:199–210. doi: 10.1016/j.jymcc.2017.11.017
50. Baher AA, Uy M, Xie F, Garfinkel A, Qu Z, Weiss JN. Bidirectional ventricular tachycardia: ping pong in the His-Purkinje system. *Heart Rhythm*. 2011;8:599–605. doi: 10.1016/j.hrthm.2010.11.038
51. Cerrone M, Noujaim SF, Talkacheva EG, Talkachou A, O'Connell R, Berenfeld O, Anumonwo J, Pandit SV, Vikstrom K, Napolitano C, et al. Arrhythmogenic mechanisms in a mouse model of catecholaminergic polymorphic ventricular tachycardia. *Circ Res*. 2007;101:1039–1048. doi: 10.1161/CIRCRESAHA.107.148064
52. Herron TJ, Milstein ML, Anumonwo J, Priori SG, Jalife J. Purkinje cell calcium dysregulation is the cellular mechanism that underlies catecholaminergic polymorphic ventricular tachycardia. *Heart Rhythm*. 2010;7:1122–1128. doi: 10.1016/j.hrthm.2010.06.010
53. Kang G, Giovannone SF, Liu N, Liu FY, Zhang J, Priori SG, Fishman GI. Purkinje cells from RyR2 mutant mice are highly arrhythmogenic but responsive to targeted therapy. *Circ Res*. 2010;107:512–519. doi: 10.1161/CIRCRESAHA.110.221481
54. Mezu UL, Singh P, Shusterman V, Hwang HS, Knollmann BC, Nemec J. Accelerated junctional rhythm and nonalternans repolarization lability precede ventricular tachycardia in Casq2-/- mice. *J Cardiovasc Electrophysiol*. 2012;23:1355–1363. doi: 10.1111/j.1540-8167.2012.02406.x
55. Pallante BA, Giovannone S, Fang-Yu L, Zhang J, Liu N, Kang G, Dun W, Boyden PA, Fishman GI. Contactin-2 expression in the cardiac Purkinje fiber network. *Circ Arrhythm Electrophysiol*. 2010;3:186–194. doi: 10.1161/CIRCEP.109.928820
56. Kocksämper J, Zima AV, Roderick HL, Pieske B, Blatter LA, Bootman MD. Emerging roles of inositol 1,4,5-trisphosphate signaling in cardiac myocytes. *J Mol Cell Cardiol*. 2008;45:128–147. doi: 10.1016/j.jymcc.2008.05.014
57. Gordienko DV, Bolton TB. Crosstalk between ryanodine receptors and IP(3) receptors as a factor shaping spontaneous Ca(2+)-release



events in rabbit portal vein myocytes. *J Physiol*. 2002;542:743–762. doi: 10.1113/jphysiol.2001.015966

58. Boyden P, Dun W, Barbhaiya C, Ter Keurs H. 2APB- and JTV519(K201)-sensitive micro Ca<sup>2+</sup> waves in arrhythmogenic Purkinje cells that survive in infarcted canine heart. *Heart Rhythm*. 2004;1:218–226. doi: 10.1016/j.hrthm.2004.03.068
59. Chung J, Tilinaité A, Ladd D, Hunt H, Soeller C, Crampin EJ, Johnston ST, Roderick HL, Rajagopal V. IP(3)R activity increases propensity of RyR-mediated sparks by elevating dyadic [Ca(2+)]. *Math Biosci*. 2023;355:108923. doi: 10.1016/j.mbs.2022.108923
60. Van Hout CV, Tachmazidou I, Backman JD, Hoffman JD, Liu D, Pandey AK, Gonzaga-Jauregui C, Khalid S, Ye B, Banerjee N, et al. Exome sequencing and characterization of 49,960 individuals in the UK Biobank. *Nature*. 2020;586:749–756. doi: 10.1038/s41586-020-2853-0
61. Bycroft C, Freeman C, Petkova D, Band G, Elliott LT, Sharp K, Motyer A, Vukcevic D, Delaneau O, O'Connell J, et al. The UK Biobank resource with deep phenotyping and genomic data. *Nature*. 2018;562:203–209. doi: 10.1038/s41586-018-0579-z
62. Boyden PA, Pu J, Pinto J, Keurs HE. Ca(2+) transients and Ca(2+) waves in purkinje cells: role in action potential initiation. *Circ Res*. 2000;86:448–455. doi: 10.1161/01.res.86.4.448
63. Boyden PA, Hirose M, Dun W. Cardiac Purkinje cells. *Heart Rhythm*. 2010;7:127–135. doi: 10.1016/j.hrthm.2009.09.017
64. Benfey BG. Function of myocardial alpha-adrenoceptors. *Life Sci*. 1990;46:743–757. doi: 10.1016/0024-3205(90)90062-v
65. Schmitz W, Eschenhagen T, Mende U, Muller FU, Scholz H. The role of alpha 1-adrenergic and muscarinic receptors in cardiac function. *Eur Heart J*. 1991;12(suppl F):83–87. doi: 10.1093/eurheartj/12.suppl.f.83
66. Kurz T, Yamada KA, DaTorre SD, Corr PB. Alpha 1-adrenergic system and arrhythmias in ischaemic heart disease. *Eur Heart J*. 1991;12(suppl F):88–98. doi: 10.1093/eurheartj/12.suppl.f.88
67. Kurtzwald-Josefson E, Hochhauser E, Bogachenko K, Harun-Khun S, Katz G, Aravot D, Seidman JG, Seidman CE, Eldar M, Shainberg A, et al. Alpha blockade potentiates CPVT therapy in calsequestrin-mutant mice. *Heart Rhythm*. 2014;11:1471–1479. doi: 10.1016/j.hrthm.2014.04.030
68. Tambeaux A, Aguilar-Sánchez Y, Santiago DJ, Mascitti M, DiNovo KM, Mejía-Alvarez R, Fill M, Wayne Chen SR, Ramos-Franco J. Ligand sensitivity of type-1 inositol 1,4,5-trisphosphate receptor is enhanced by the D2594K mutation. *Pflugers Arch*. 2023;475:569–581. doi: 10.1007/s00424-023-02796-x
69. Ho SN, Hunt HD, Horton RM, Pullen JK, Pease LR. Site-directed mutagenesis by overlap extension using the polymerase chain reaction [see comments]. *Gene*. 1989;77:51–59. doi: 10.1016/0378-1119(89)90358-2
70. Suzuki J, Kanemaru K, Ishii K, Ohkura M, Okubo Y, Iino M. Imaging intracellular Ca<sup>2+</sup> at subcellular resolution using CEPIA. *Nat Commun*. 2014;5:4153. doi: 10.1038/ncomms5153
71. Sun B, Ni M, Tian S, Guo W, Cai S, Sondergaard MT, Chen Y, Mu Y, Estillore JP, Wang R, et al. A gain-of-function mutation in the ITPR1 gating domain causes male infertility in mice. *J Cell Physiol*. 2022;237:3305–3316. doi: 10.1002/jcp.30783
72. Yao J, Ni M, Tian S, Sun B, Wang R, Estillore JP, Back TG, Chen SRW. A gain-of-function mutation in the gating domain of ITPR1 impairs motor movement and increases thermal and mechanical sensitivity. *Neuroscience*. 2023;522:11–22. doi: 10.1016/j.neuroscience.2023.04.031
73. Wang K, Terrar D, Gavaghan DJ, Mu UMR, Kohl P, Bollensdorff C. Living cardiac tissue slices: an organotypic pseudo two-dimensional model for cardiac biophysics research. *Prog Biophys Mol Biol*. 2014;115:314–327. doi: 10.1016/j.pbiomolbio.2014.08.006
74. Pallante BA, Giovannone S, Fang-Yu L, Zhang J, Liu N, Kang G, Dun W, Boyden PA, Fishman GI. Contactin-2 expression in the cardiac Purkinje fiber network. *Circ Arrhythm Electrophysiol*. 2010;3:186–194. doi: 10.1161/CIRCEP.109.928820
75. Kang G, Giovannone SF, Liu N, Liu FY, Zhang J, Priori SG, Fishman GI. Purkinje cells from RyR2 mutant mice are highly arrhythmogenic but responsive to targeted therapy. *Circ Res*. 2010;107:512–519. doi: 10.1161/CIRCRESAHA.110.221481
76. Zhou Q, Xiao J, Jiang D, Wang R, Vembaiyan K, Wang A, Smith CD, Xie C, Chen W, Zhang J, et al. Carvedilol and its new analogs suppress arrhythmogenic store overload-induced Ca<sup>2+</sup> release. *Nat Med*. 2011;17:1003–1009. doi: 10.1038/nm.2406
77. Tomek J, Nieves-Cintrón M, Navedo MF, Ko CY, Bers DM. SparkMaster 2: a new software for automatic analysis of calcium spark data. *Circ Res*. 2023;133:450–462. doi: 10.1161/CIRCRESAHA.123.322847
78. Varro A, Negretti N, Hester SB, Eisner DA. An estimate of the calcium content of the sarcoplasmic reticulum in rat ventricular myocytes. *Pflugers Arch*. 1993;423:158–160. doi: 10.1007/BF00374975
79. Daniels RE, Haq KT, Miller LS, Chia EW, Miura M, Sorrentino V, McGuire JJ, Stuyvers BD. Cardiac expression of ryanodine receptor subtype 3; a strategic component in the intracellular Ca(2+) release system of Purkinje fibers in large mammalian heart. *J Mol Cell Cardiol*. 2017;104:31–42. doi: 10.1016/j.yjmcc.2017.01.011
80. Cerrone M, Colombi B, Santoro M, di Barletta MR, Scelsi M, Villani L, Napolitano C, Priori SG. Bidirectional ventricular tachycardia and fibrillation elicited in a knock-in mouse model carrier of a mutation in the cardiac ryanodine receptor. *Circ Res*. 2005;96:e77–e82. doi: 10.1161/01.RES.0000169067.51055.72
81. Chen B, Guo A, Gao Z, Wei S, Xie YP, Chen SR, Anderson ME, Song LS. In situ confocal imaging in intact heart reveals stress-induced Ca(2+) release variability in a murine catecholaminergic polymorphic ventricular tachycardia model of type 2 ryanodine receptor(R4496C+/-) mutation. *Circ Arrhythm Electrophysiol*. 2012;5:841–849. doi: 10.1161/CIRCEP.111.969733
82. Zhang J, Zhou Q, Smith CD, Chen H, Tan Z, Chen B, Nani A, Wu G, Song LS, Fill M, et al. Non-beta-blocking R-carvedilol enantiomer suppresses Ca<sup>2+</sup> waves and stress-induced ventricular tachyarrhythmia without lowering heart rate or blood pressure. *Biochem J*. 2015;470:233–242. doi: 10.1042/BJ20150548
83. Bycroft C, Freeman C, Petkova D, Band G, Elliott LT, Sharp K, Motyer A, Vukcevic D, Delaneau O, O'Connell J, et al. The UK Biobank resource with deep phenotyping and genomic data. *Nature*. 2018;562:203–209. doi: 10.1038/s41586-018-0579-z
84. McLaren W, Gil L, Hunt SE, Riat HS, Ritchie GR, Thormann A, Flicek P, Cunningham F. The Ensembl variant effect predictor. *Genome Biol*. 2016;17:122. doi: 10.1186/s13059-016-0974-4
85. Rohde PD, Fourie Sørensen I, Sørensen P. qgg: an R package for large-scale quantitative genetic analyses. *Bioinformatics*. 2020;36:2614–2615. doi: 10.1093/bioinformatics/btz955
86. Zhong X, Sun B, Vallmitjana A, Mi T, Guo W, Ni M, Wang R, Guo A, Duff HJ, Gillis AM, et al. Suppression of ryanodine receptor function prolongs Ca<sup>2+</sup> release refractoriness and promotes cardiac alternans in intact hearts. *Biochem J*. 2016;473:3951–3964. doi: 10.1042/BCJ20160606
87. Sikkel MB, Francis DP, Howard J, Gordon F, Rowlands C, Peters NS, Lyon AR, Harding SE, MacLeod KT. Hierarchical statistical techniques are necessary to draw reliable conclusions from analysis of isolated cardiomyocyte studies. *Cardiovasc Res*. 2017;113:1743–1752. doi: 10.1093/cvr/cvx151
88. Casey JP, Hirouchi T, Hisatsune C, Lynch B, Murphy R, Dunne AM, Miyamoto A, Ennis S, van der Spek N, O'Hici B, et al. A novel gain-of-function mutation in the ITPR1 suppressor domain causes spinocerebellar ataxia with altered Ca<sup>2+</sup> signal patterns. *J Neurol*. 2017;264:1444–1453. doi: 10.1007/s00415-017-8545-5
89. Synofzik M, Helbig KL, Harmuth F, Deconinck T, Tanpaiboon P, Sun B, Guo W, Wang R, Palmaer E, Tang S, et al. De novo ITPR1 variants are a recurrent cause of early-onset ataxia, acting via loss of channel function. *Eur J Hum Genet*. 2018;26:1623–1634. doi: 10.1038/s41431-018-0206-3
90. Sasaki M, Ohba C, Iai M, Hirabayashi S, Osaka H, Hiraide T, Saitou H, Matsumoto N. Sporadic infantile-onset spinocerebellar ataxia caused by missense mutations of the inositol 1,4,5-trisphosphate receptor type 1 gene. *J Neurol*. 2015;262:1278–1284. doi: 10.1007/s00415-015-7705-8
91. Wang T, Guo H, Xiong B, Stessman HAF, Wu H, Coe BP, Turner TN, Liu Y, Zhao W, Hoekzema K, et al. De novo genic mutations among a Chinese autism spectrum disorder cohort. *Nat Commun*. 2016;7:13316. doi: 10.1038/ncomms13316